of AM may also improve established emphysema at least in part through mobilization of bone marrow cells and their differentiation into alveolar epithelial cells and vascular endothelial cells.

This study includes a study limitation. We used an elastase-induced model of emphysema to demonstrate that AM has the capacity to promote regeneration of alveoli and vasculature. An elastase-induced model is often used because of its relative simplicity and particularly useful for investigating mechanisms of lung repair. However, the artificiality of putting a large amount of elastase into the animal lung limits the usefulness of this model in answering questions relating to mechanisms of human emphysema. Moreover, cigarette smoke exposure causes a variety of other abnormalities that are not observed with simple intratracheal instillation of elastase. Thus, the results obtained from the elastase model may not be predictive of response to therapy in human cigarette smoke–induced pulmonary emphysema. Therefore, the initial success of AM therapy reported here should be confirmed by further studies using other animal models of pulmonary emphysema before clinical trials.

In conclusion, continuous infusion of AM improved elastase-induced emphysema. These beneficial effects of AM may be mediated at least in part through mobilization of bone marrow cells and the direct protective effects on alveolar epithelial cells and endothelial cells. Thus, this may be a new therapeutic strategy for the treatment of pulmonary emphysema.

Conflict of Interest Statement: None of the authors have a financial relationship with a commercial entity that has an interest in the subject of this manuscript.

Acknowledgment: The authors thank Prof. Masaru Okabe for providing us with transgenic mice that ubiquitously express green fluorescent protein, and Yuki Isono, Aki Nogimori, and Natue Sakata for their excellent technical assistance.

References

1. Lopez AD, Murray CC. The global burden of disease, 1990–2020. *Nat Med* 1998;4:1241–1243.
2. Croxton TL, Weinmann GG, Senior RM, Wise RA, Crapo JD, Buist AS. Clinical research in chronic obstructive pulmonary disease: needs and opportunities. *Am J Respir Crit Care Med* 2003;167:1142–1149.
3. American Thoracic Society. Standards for the diagnosis and care of patients with chronic obstructive pulmonary disease. *Am J Respir Crit Care Med* 1995;152:S77–S121.
4. Ishizawa K, Kubo H, Yamada M, Kobayashi S, Numasaki M, Ueda S, Suzuki T, Sasaki H. Bone marrow-derived cells contribute to lung regeneration after elastase-induced pulmonary emphysema. *FEBS Lett* 2004;556:249–252.
5. Yamada M, Kubo H, Kobayashi S, Ishizawa K, Numasaki M, Ueda S, Suzuki T, Sasaki H. Bone marrow-derived progenitor cells are important for lung repair after lipopolysaccharide-induced lung injury. *J Immunol* 2004;172:1266–1272.
6. Kitamura K, Kangawa K, Kawamoto M, Ichiki Y, Nakamura S, Matsuo H, Eto T. Adrenomedullin: a novel hypotensive peptide isolated from human pheochromocytoma. *Biochem Biophys Res Commun* 1993;192: 553–560.
7. Ichiki Y, Kitamura K, Kangawa K, Kawamoto M, Matsuo H, Eto T. Distribution and characterization of immunoreactive adrenomedullin in human tissue and plasma. *FEBS Lett* 1994;338:6–10.
8. Sakata J, Shimokubo T, Kitamura K, Nishizono M, Iehiki Y, Kangawa K, Matsuo H, Eto T. Distribution and characterization of immunoreactive rat adrenomedullin in tissue and plasma. *FEBS Lett* 1994;352:105–108.
9. Martinez A, Miller MJ, Catt KJ, Cuttitta F. Adrenomedullin receptor expression in human lung and in pulmonary tumors. *J Histochem Cytochem* 1997;45:159–164.
10. Nishimatsu H, Suzuki E, Nagata D, Moriyama N, Satonaka H, Walsh K, Sata M, Kangawa K, Matsuo H, Goto A, *et al.* Adrenomedullin induces endothelium-dependent vasorelaxation via the phosphatidylinositol 3-kinase/Akt-dependent pathway in rat aorta. *Circ Res* 2001;891:63–70.
11. Shiojima I, Walsh K. Role of Akt signaling in vascular homeostasis and angiogenesis. *Circ Res* 2002;90:1243–1250.
12. Kim W, Moon SO, Sung MJ, Kim SH, Lee S, So JN, Park SK. Angiogenic role of adrenomedullin through activation of Akt, mitogen-activated protein kinase, and focal adhesion kinase in endothelial cells. *FASEB J* 2003;17:1937–1939.
13. Tokunaga N, Nagaya N, Shirai M, Tanaka E, Ishibashi-Ueda H, Harada-Shiba M, Kanda M, Ito T, Shimizu W, Tabata Y, *et al.* Adrenomedullin gene transfer induces therapeutic angiogenesis in a rabbit model of chronic hind limb ischemia: benefits of a novel nonviral vector, gelatin. *Circulation* 2004;109:526–531.
14. Okabe M, Ikawa M, Kominami K, Nakanishi T, Nishimune Y. 'Green mice' as a source of ubiquitous green cells. *FEBS Lett* 1997;407:313–319.
15. Massaro GD, Massaro D. Retinoic acid treatment abrogates elastase-induced pulmonary emphysema in rats. *Nat Med* 1997;3:675–677.
16. Asahara T, Takahashi T, Masuda H, Kalka C, Chen D, Iwaguro H, Inai Y, Silver M, Isner JM. VEGF contributes to postnatal neovascularization by mobilizing bone marrow-derived endothelial progenitor cells. *EMBO J* 1999;18:3964–3972.
17. Sata M, Saiura A, Kunisato A, Tojo A, Okada S, Tokuhisa T, Hirai H, Makuuchi M, Hirata Y, Nagai R. Hematopoietic stem cells differentiate into vascular cells that participate in the pathogenesis of atherosclerosis. *Nat Med* 2002;8:403–409.
18. Scherle W. A simple method for volumetry of organs in quantitative stereology. *Mikroskopie* 1970;26:57–60.
19. Thurlbeck WM. Internal surface area and other measurements in emphysema. *Thorax* 1967;22:483–496.
20. Itoh T, Nagaya N, Murakami S, Fujii T, Iwase T, Ishibashi-Ueda H, Yutani C, Yamagishi M, Kimura H, Kangawa K. C-type natriuretic peptide ameliorates monocrotaline-induced pulmonary hypertension in rats. *Am J Respir Crit Care Med* 2004;170:1204–1211.
21. Nakajoh M, Fukushima T, Suzuki T, Yamaya M, Nakayama K, Sekizawa K, Sasaki H. Retinoic acid inhibits elastase-induced injury in human lung epithelial cell lines. *Am J Respir Cell Mol Biol* 2003;28:296–304.
22. Aicher A, Heeschen C, Mildner-Rihm C, Urbich C, Ihling C, Technau-Ihling K, Zeiher AM, Dimmeler S. Essential role of endothelial nitric oxide synthase for mobilization of stem and progenitor cells. *Nat Med* 2003;9:1370–1376.
23. Shimekake Y, Nagata K, Ohta S, Kambayashi Y, Teraoka H, Kitamura K, Eto T, Kangawa K, Matsuo H. Adrenomedullin stimulates two signal transduction pathways, cAMP accumulation and Ca2+ mobilization, in bovine aortic endothelial cells. *J Biol Chem* 1995;270:4412–4417.
24. Nagaya N, Satoh T, Nishikimi T, Uematsu M, Furuichi S, Sakamaki F, Oya H, Kyotani S, Nakanishi N, Goto Y, *et al.* Hemodynamic, renal, and hormonal effects of adrenomedullin infusion in patients with congestive heart failure. *Circulation* 2000;101:498–503.
25. Kato H, Shichiri M, Marumo F, Hirata Y. Adrenomedullin as an autocrine/paracrine apoptosis survival factor for rat endothelial cells. *Endocrinology* 1997;138:2615–2620.
26. Sata M, Kakoki M, Nagata D, Nishimatsu H, Suzuki E, Aoyagi T, Sugiura S, Kojima H, Nagano T, Kangawa K, *et al.* Adrenomedullin and nitric oxide inhibit human endothelial cell apoptosis via a cyclic GMP-independent mechanism. *Hypertension* 2000;36:83–88.
27. Kano H, Kohno M, Yasunari K, Yokokawa K, Horio T, Ikeda M, Minami M, Hanehira T, Takeda T, Yoshikawa J. Adrenomedullin as a novel antiproliferative factor of vascular smooth muscle cells. *J Hypertens* 1996;14:209–213.
28. Kitamura K, Kangawa K, Eto T. Adrenomedullin and PAMP: discovery, structures, and cardiovascular functions. *Microsc Res Tech* 2002;57: 3–13.
29. Asahara T, Murohara T, Sullivan A, Silver M, van der Zee R, Li T, Witzenbichler B, Schatteman G, Isner JM. Isolation of putative progenitor endothelial cells for angiogenesis. *Science* 1997;275:964–967.
30. Moore MA, Hattori K, Heissig B, Shieh JH, Dias S, Crystal RG, Rafii S. Mobilization of endothelial and hematopoietic stem and progenitor cells by adenovector-mediated elevation of serum levels of SDF-1, VEGF, and angiopoietin-1. *Ann N Y Acad Sci* 2001;938:36–45.
31. Heissig B, Hattori K, Dias S, Friedrich M, Ferris B, Hackett NR, Crystal RG, Besmer P, Lyden D, Moore MA, *et al.* Recruitment of stem and progenitor cells from the bone marrow niche requires MMP-9 mediated release of kit-ligand. *Cell* 2002;109:625–637.
32. Gu Z, Kaul M, Yan B, Kridel SJ, Cui J, Strongin A, Smith JW, Liddington RC, Lipton SA. S-nitrosylation of matrix metalloproteinases: signaling pathway to neuronal cell death. *Science* 2002;297:1186–1190.
33. Shintani S, Murohara T, Ikeda H, Ueno T, Honma T, Katoh A, Sasaki K, Shimada T, Oike Y, Imaizumi T. Mobilization of endothelial progenitor cells in patients with acute myocardial infarction. *Circulation* 2001;103:2776–2779.
34. Tateishi-Yuyama E, Matsubara H, Murohara T, Ikeda U, Shintani S,

Masaki H, Amano K, Kishimoto Y, Yoshimoto K, Akashi H, *et al.* Therapeutic angiogenesis for patients with limb ischaemia by autologous transplantation of bone-marrow cells: a pilot study and a randomised controlled trial. *Lancet* 2002;360:427–435.
35. Snider GL, Lucey EC, Stone PJ. Animal models of emphysema. *Am Rev Respir Dis* 1986;133:149–169.
36. Hayes JA, Korthy A, Snider GL. The pathology of elastase-induced panacinar emphysema in hamsters. *J Pathol* 1975;117:1–14.
37. Kuraki T, Ishibashi M, Takayama M, Shiraishi M, Yoshida M. A novel oral neutrophil elastase inhibitor (ONO-6818) inhibits human neutrophil elastase-induced emphysema in rats. *Am J Respir Crit Care Med* 2002;166:496–500.
38. Miyashita K, Itoh H, Sawada N, Fukunaga Y, Sone M, Yamahara K, Yurugi T, Nakao K. Adrenomedullin promotes proliferation and migration of cultured endothelial cells. *Hypertens Res* 2003;26:S93–S98.
39. Rennard SI. Inflammation and repair processes in chronic obstructive pulmonary disease. *Am J Respir Crit Care Med* 1999;160:S12–S16.
40. Wang H, Liu X, Umino T, Skold CM, Zhu Y, Kohyama T, Spurzem JR, Romberger DJ, Rennard SI. Cigarette smoke inhibits human bronchial epithelial cell repair processes. *Am J Respir Cell Mol Biol* 2001;25:772–779.
41. Kasahara Y, Tuder RM, Taraseviciene-Stewart L, Le Cras TD, Abman S, Hirth PK, Waltenberger J, Voelkel NF. Inhibition of VEGF receptors causes lung cell apoptosis and emphysema. *J Clin Invest* 2000;106:1311–1319.
42. Kasahara Y, Tuder RM, Cool CD, Lynch DA, Flores SC, Voelkel NF. Endothelial cell death and decreased expression of vascular endothelial growth factor and vascular endothelial growth factor receptor 2 in emphysema. *Am J Respir Crit Care Med* 2001;163:737–744.

ELSEVIER

Atherosclerosis 185 (2006) 165–172

ATHEROSCLEROSIS

www.elsevier.com/locate/atherosclerosis

Altered expression balance of matrix metalloproteinases and their inhibitors in human carotid plaque disruption: Results of quantitative tissue analysis using real-time RT-PCR method

Takeo Higashikata [a], Masakazu Yamagishi [a,*], Toshio Higashi [b], Izumi Nagata [b], Koji Iihara [b], Susumu Miyamoto [b], Hatsue Ishibashi-Ueda [c], Noritoshi Nagaya [d], Takashi Iwase [d], Hitonobu Tomoike [a], Aiji Sakamoto [e]

[a] *Division of Cardiovascular Medicine and Bioscience, National Cardiovascular Center and Research Institute, 5-7-1 Fujishiro-dai, Suita, Osaka 565-8565, Japan*

[b] *Division of Neurosurgery, National Cardiovascular Center, Suita, Osaka, Japan*

[c] *Division of Pathology, National Cardiovascular Center, Suita, Osaka, Japan*

[d] *Division of Regenerative Medicine and Tissue Engineering, National Cardiovascular Center and Research Institute, Suita, Osaka, Japan*

[e] *Division of Biotechnology and Bioscience, National Cardiovascular Center and Research Institute, Suita, Osaka, Japan*

Received 28 October 2004; received in revised form 17 May 2005; accepted 27 May 2005
Available online 21 July 2005

Abstract

Background: The balance between degradation and synthesis of extracellular matrix determines its content in atherosclerotic tissue. To examine the role of expression balance of matrix metalloproteinases (MMPs) to their inhibitors, tissue inhibitors of metalloproteinases (TIMPs) and tissue factor pathway inhibitor-2 (TFPI-2) in the development and disruption of atherosclerotic plaque, these gene expressions in human carotid plaque were quantitatively determined by real-time reverse transcription (RT)-polymerase chain reaction (PCR) method.
Methods: Total RNA for cDNA synthesis was extracted from tissues in 24 patients with carotid endarterectomy. The amounts of cDNAs for MMP-1, -2, -3 and -9, TFPI-2 and TIMP-1, -2 and -3 were determined by real-time RT-PCR method, and normalized with glutaraldehyde 3-dehydrogenase.
Results: In plaques, the expression MMP-1 (1.53 ± 0.25, mean ± S.E.M.), MMP-3 (1.99 ± 0.59) and MMP-9 (2.00 ± 0.51) was augmented compared to those in the adjacent control regions (0.60 ± 0.16, 0.46 ± 0.18 and 0.58 ± 0.21, respectively, $p < 0.05$). The expression of TFPI-2 was lower in plaques (0.32 ± 0.08) than in controls (0.94 ± 0.23, $p < 0.01$). Although the expression of TIMP-1 was higher in plaques (1.28 ± 0.23) than in controls (0.81 ± 0.10, $p < 0.05$), the indices of MMP-1/TIMP-1, MMP-3/TIMP-3 and MMP-9/TIMP-1 were still significantly higher in plaques. Interestingly, MMP-9 and the resulting MMP-9/TIMP-1 balance in plaques with disruption were significantly higher (3.36 ± 1.52 and 1.66 ± 0.12, $n = 11$) than those in non-disrupted plaques (1.11 ± 0.52 and 0.76 ± 0.12, $n = 13$, $p < 0.05$).
Conclusion: With the decreased expression of TFPI-2, upregulation of MMPs in atherosclerotic plaque was disproportional to that of TIMPs, suggesting that imbalanced degradation and synthesis of extracellular matrix persists in advanced lesions, particularly in plaques with disruption.

Keywords: Atherosclerosis; Extracellular matrix; Matrix metalloproteinases; Tissue inhibitor of metalloproteinases; Tissue factor pathway inhibitor-2; Plaque disruption

1. Introduction

Disruption of atherosclerotic plaque during its development can expose the thrombogenic core to luminal blood flow, frequently resulting in ischemic cardiac events and stroke

* Corresponding author. Tel.: +81 6 6833 5012; fax: +81 6 6833 9865.
E-mail address: myamagi@hsp.ncvc.go.jp (M. Yamagishi).

0021-9150/$ – see front matter © 2005 Elsevier Ireland Ltd. All rights reserved.
doi:10.1016/j.atherosclerosis.2005.05.039

[1,2]. During this process, structural changes in extracellular matrix (ECM) were shown to play a crucial role in plaque development and disruption [3]. The structural integrity of plaques seems to depend on a balance between synthesis and degradation of the ECM which is mainly regulated by proteinases such as matrix metalloproteinases (MMPs) including interstitial collagenase or MMP-1, gelatinase A or MMP-2, stromelysin 1 or MMP-3, gelatinase B or MMP-9 [4,5].

The activities of MMPs are controlled on multiple levels: transcription and translation of their inactive precursors (zymogens), post-translational activation of zymogens by proteolysis and interactions with tissue inhibitors of metalloproteinases (TIMPs) [6] and/or tissue factor pathway inhibitor-2 (TFPI-2) [7]. Indeed, TIMPs-1, -2, -3 and TFPI-2 are expressed in atherosclerotic lesions [7–9], and these inhibitors bind to and inactivate most of the MMPs [7,10]. Thus, the expression balance of MMP to TIMP and TFPI-2 is considered to regulate the net degeneration of ECM, thus contributing to maintaining plaque stability [7,11,12]. However, few systematic data exist regarding quantitative evaluation of the expression of MMPs and their inhibitors in human atherosclerotic plaques, probably because of technical difficulties in simultaneous determination of multiple gene expression in small tissue samples obtained in clinical settings. In the present study, we used real-time reverse transcription (RT)-polymerase chain reaction (PCR) and analyzed gene expression levels of MMPs, TIMPs and TFPI-2 in human carotid plaque and an adjacent control region. We also compared expression and function of MMPs between histologically disrupted and non-disrupted plaques.

2. Subjects and methods

2.1. Subjects

The protocol of this study was approved by the institutional committee for ethical review. Written informed consent was obtained from all 24 patients who underwent carotid endarterectomy for severe stenosis of the extracranial carotid artery (all male with mean age of 68 ± 2 years). All patients presented clinical symptoms of cerebral ischemic attack related to carotid stenosis. Seven patients had a history of recent ischemic attack within 1 month prior to endarterectomy. The prevalence of risk factors for atherosclerosis was as follows: hypertension (systolic pressure >160 mmHg) in 20, hyperlipidemia (total cholesterol >220 mg/dl) in 22, smoking in 15 and diabetes mellitus (fasting blood glucose >110 mg/dl) in 10 patients. High sensitive (hs) CRP level (normal range <3 mg/l) just before surgery was 2.45 ± 0.43 mg/l (Table 1).

2.2. Tissue sampling

Samples of the plaque region were obtained immediately after endarterectomy. Endarterectomy was extended in a caudal direction to include a sample of minimally affected common carotid artery proximal to the plaque but in continuity with the plaque to act as a paired control. Under these conditions, the stenotic segment and adjacent areas were dissected undisruptedly as a single specimen, preserving circumferential integrity as much as possible. Also special care was taken not to damage luminal surface and plaque interior. After removing a part of the tissue for histological examination, all samples were immediately frozen in liquid nitrogen and stored at −80 °C until extraction of mRNA.

Procedures for RNA preparation and cDNA synthesis were already described elsewhere in detail [13]. Briefly, the samples were homogenized in 1.0 ml ISOGEN™ reagent (Nippon Gene, Tokyo, Japan), thoroughly mixed with 0.2 ml chloroform and centrifuged at 15,000 × *g* for 15 min at 4 °C. The aqueous supernatant was transferred into a micro test tube, mixed with 0.6 ml isopropanol and centrifuged at 15,000 × *g* for 15 min at 4 °C. The precipitated total RNA was rinsed with 70% ethanol, air-dried and then resuspended in RNase-free water. Then, all the total RNA was treated with DNase Free™ reagent (Ambion, Austin, TX) for 60 min, and then reverse-transcribed with Superscript II™ (Invitrogen, Carlsbad, CA) at 37 °C for 60 min using random primers (TaKaRa, Tokyo, Japan). The integrity of each cDNA mixture was checked by amplification of glutaraldehyde 3-phosphate dehydrogenase (GAPDH) with *ExTaq* (TaKaRa), using the primer set 5′-ACCACAGTCCATGCCATCAC-3′/5′-TCCACCACCCTGTTGCTGTA-3′.

Table 1
Patient Characteristics

	All patients ($n = 24$)	With disruption ($n = 11$)	Without disruption ($n = 13$)	p-Value
Age	68 ± 2	66 ± 3	69 ± 2	NS
Male sex	24	11	13	NS
Hypertension	20	8	12	NS
Diabetes	10	5	5	NS
HbA1c (%)	6.5 ± 0.4	7.0 ± 0.8	6.2 ± 0.4	NS
Hyperlipidemia	22	9	13	NS
LDL (mg/dl)	132 ± 6	140 ± 10	128 ± 7	NS
Smoking	15	5	10	NS
hs-CRP (mg/l)	2.45 ± 0.43	2.68 ± 0.49	2.12 ± 0.81	NS

2.3. Primers and probes for real-time RT-PCR

Using Primer Express™ software (Applied Biosystems, Foster, CA), primers were designed for each of the genes for MMP-1, -2, -3 and -9, TFPI-2 and TIMP-1, -2 and -3, and the TaqMan probe inherent to each primer set was prepared, which was an oligonucleotide labeled with a reporter dye (FAM) at the 5′-end and a quencher dye (TAMRA) at the 3′-end. The sequences of the primers and TaqMan probes of MMPs-1, -2, -3, -9, TIMPs-1, -2 and -9 were reported elsewhere [13], and those for TFPI-2 were SENSE = CGATGCTTGCTGGAGGATAGA; ANTISENSE = ACACTGGTCGTCCACACTCACT; Taqman probe = 5′-FAM-AAGTTCCCAAAGTTTGCCGGCTGC-TAMRA-3′; TFPI-2 SENSE = CGATGCTTGCTGGAGGATAGA; ANTISENSE = ACACTGGTCGTCCACACTCACT; Taqman probe = 5′-FAM-AAGTTCCCAAAGTTTGCCGGCTGC-TAMRA-3′.

Real-time RT-PCR was performed using an ABI PRISM 7700 Sequence Detection System (Applied Biosystems). The reaction solution was assembled in a volume of 25 μl, which comprised TaqMan Universal PCR Master Mix (Applied Biosystems), forward and reverse primers (final concentration 300 nM each), TaqMan probe (final concentration 200 nM) and cDNA mixture (about 2.5 ng). Throughout this study, the cDNA mixture from a particular sample was used to generate the working standard for quantitation of the cDNA of interest, which plots the relationship between the dilution of the standard cDNAs and the corresponding C_t value (the number of cycles necessary to obtain a threshold fluorescent signal) [13]. The initial quantity of the cDNA of interest in a certain cDNA mixture was calculated from the working standard and then normalized to that of GAPDH determined with TaqMan Assay Reagent Endogenous Control™ (Applied Biosystems). The normalized value for each target cDNA reflects the expression level of the corresponding gene in a test sample relative to the standard tissue. The accuracy of the present real-time RT-PCR for determining mRNA expression in human vascular tissue was already confirmed by comparing the results with those determined by conventional RT-PCR method [13].

2.4. Expression and function of MMP

To determine expression and function of MMP in its protein level, carotid tissue samples from 10 patients, in whom enough amounts of proteins could be extracted, were examined by Western blotting and gel zymography. The extracted protein was separated by SDS-PAGE and blotted onto a Hybond-ECL nitrocellulose membrane (Amersham) with the use of primary (40 μg/ml) and secondary (1:2000, Amersham) antibodies. As for zymography, proteins with gelatinolytic activity were identified by use of substrate gels prepared by incorporation of gelatin (1 mg/ml; Wako) into a SDS-PAGE. After elecrophoresis, gels were washed in 2.5% Triton X-100 for 30 min to remove SDS. The gel was equilibrated for 30 min at room temperature with gentle agitation then incubated for overnight at 37 °C in 50 mM Tris/HCl, pH 7.5, containing 0.2 M NaCl, 5 mM $CaCl_2$ and 0.02% Brij 35. Gels were then fixed and stained with 0.25% Coomassie Brilliant Blue R-250 (Wako). The product of the optical net density of the band was compared with a positive control (HT-1080 human fibrosarcoma cells for Western blotting and human MMP-2 and human MMP-9, 1.5 ng, CC073; CHEMICON for zymography) to obtain a ratio comparable between gels.

2.5. Histology and immunohistochemistry

A part of the plaque was placed in tissue fixative (Histochoice, Hedwin, Baltimore). After overnight fixation, the samples were paraffin embedded and sectioned at 4-μm intervals. Tissue sections were deparaffinized with xylene followed by immersion in graded alcohol. They were washed three times for 5 min each in phosphate-buffered saline (PBS) and blocked with bovine serum albumin for 60 min. Specimens were then incubated with primary antibodies against CD-68, MMPs, TIMPs and TFPI-2 (Fuji Chemical, Tokyo, Japan) overnight at 4 °C. After they were washed in PBS, specimens were incubated with biotinylated rabbit anti-mouse IgG for 60 min at room temperature. Specimens were then washed with PBS, stained with horseradish peroxidase-conjugated streptavidin, and finally incubated with substrate solution for 1–15 min. The tissue sections were also stained with hematoxylin–eosin and elastica van Gieson for evaluation of plaque composition and fibrous cap disruption, as described by Carr et al. [2]. Plaque was defined as atheromatous if the area of lipid core was ≥30% of the whole plaque area and as fibrous plaque if <30% in terms of its vulnerability [14].

2.6. Data analysis

The mean and standard error of triplicate data are presented. Statistical analysis was performed by paired *t*-test using Stat View 5.0 software on a Macintosh computer and by Wilcoxon matched-pair signed-rank test if appropriate. A p-value <0.05 was considered significant.

3. Results

3.1. Patient and plaque characteristics

Atheromatous plaque was observed in 15 samples and fibrous plaque in 9 samples. Disruption of the fibrous cap was observed in 11 samples with atheromatous plaque and was not observed in 13 samples, which consisted of 4 atheromatous and 9 fibrous plaques. Although levels of HbA1c and LDL-cholesterol in patients with plaque disruption tended to be higher than those in patients without disruption, there was no statistically significant difference in their clinical back-

Table 2
MMP, TFPI-2 and TIMP levels

Mrna	Control	Plaque	p-Value
MMP-1	0.60 ± 0.16	1.53 ± 0.25	<0.01
MMP-2	0.80 ± 0.11	0.88 ± 0.14	NS
MMP-3	0.46 ± 0.18	1.99 ± 0.59	<0.05
MMP-9	0.58 ± 0.21	2.00 ± 0.51	<0.01
TFPI-2	0.94 ± 0.23	0.32 ± 0.08	<0.01
TIMP-1	0.81 ± 0.10	1.28 ± 0.23	<0.05
TIMP-2	1.12 ± 0.15	0.95 ± 0.17	NS
TIMP-3	0.47 ± 0.16	0.67 ± 0.17	NS

ground. Also there was no difference in hs-CRP level between two patient groups, although mean value in all patients was higher than normal value (Table 1).

3.2. Expression levels of MMPs, TIMPs and TFPI-2

From removed samples with a wet weight of 11.69 ± 2.64 mg, 0.49 ± 0.22 μg total RNA was extracted for analysis. Amplification of GAPDH was equivalent among all the cDNAs synthesized. Each primer set for PCR exponentially amplified its target cDNA according to the cycle number. Normalized values for MMP, TIMP and TFPI-2 gene expression in plaque and adjacent control tissue (controls) are summarized in Table 2. In the plaques, the gene expression levels of MMP-1 (1.53 ± 0.25), MMP-3 (1.99 ± 0.59) and MMP-9 (2.00 ± 0.51) were significantly higher than those in the controls (0.60 ± 0.16, 0.46 ± 0.18 and 0.58 ± 0.21, respectively, $p < 0.05$). However, no difference was found in the expression level of MMP-2 gene between the plaques and controls (0.88 ± 0.14 versus 0.80 ± 0.11). It was quite interesting that TFPI-2 gene expression was significantly higher in the controls (0.94 ± 0.23) than that in plaques (0.32 ± 0.08, $p < 0.01$).

As for TIMP genes, the only TIMP-1 gene was significantly upregulated in plaques in comparison with that in the controls (1.28 ± 0.23 versus 0.81 ± 0.10, $p < 0.05$) (Table 2). Among the combination of the ratios of the four MMPs to the three TIMPs examined in this study, the expression ratios of MMP-1 to TIMP-1, MMP-3 to TIMP-3 and MMP-9 to TIMP-1 were significantly higher in plaques than in the controls (2.98 ± 0.77 versus 0.99 ± 0.43, 2.18 ± 0.53 versus 0.63 ± 0.22 and 1.80 ± 0.14 versus 0.83 ± 0.09, respectively, $p < 0.05$) (Fig. 1). Of interest, in plaques with disruption of fibrous cap, MMP-9 expression (3.36 ± 1.52) and the ratio of MMP-9 to TIMP-1 (1.66 ± 0.12) were significantly higher than those in plaques without disruption (1.11 ± 0.52 and 0.76 ± 0.12, respectively), although TFPI-2 gene expression was not different between these groups (0.27 ± 0.08 versus 0.40 ± 0.18).

MMP-9 protein was expressed both in disrupted and non-disrupted plaques, but was not expressed or only slightly expressed in controls. Under these conditions, net expression of MMP-9 was significantly higher in disrupted (2.61 ± 0.17,

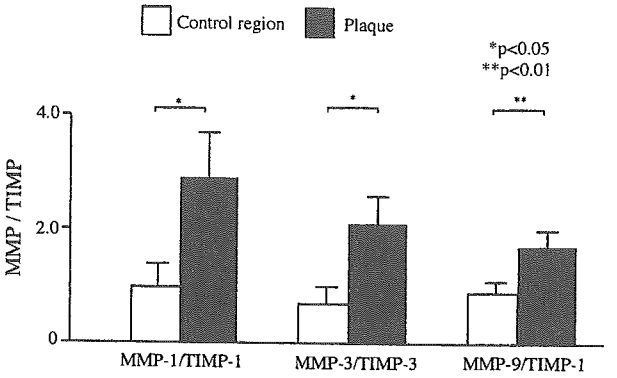

Fig. 1. Imbalanced expression of matrix metalloproteinase (MMP) to tissue inhibitor of matrix metalloproteinase (TIMP) genes in carotid plaque. Vertical axis represented the ratio of MMP/TIMP. Open columns represent values from control regions and closed columns values from plaques.

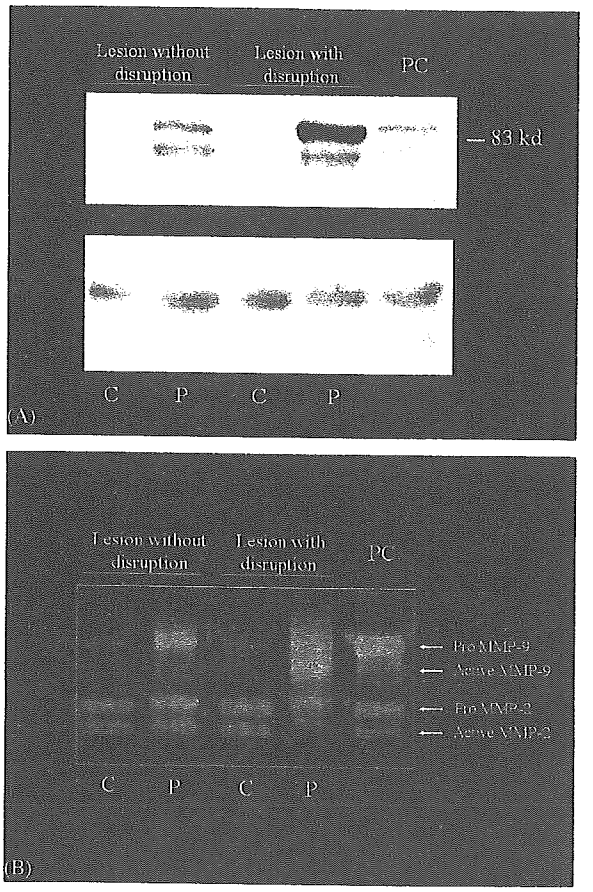

Fig. 2. Expression and function of MMP-9 in protein level. (A) Western blotting for matrix metalloproteinase MMP-9 (upper) and an internal marker protein, endothelin receptor (ETR) (lower), in non-ruptured lesion, ruptured carotid lesions and positive control (PC). MMP-9 was clearly expressed in the plaque (P) and PC, whereas in the control region (C), little expression of MMP-9 was observed. Note that both pro* and active** form of MMP-9 appears to be highly expressed in the ruptured plaque, in comparison with the non-ruptured plaque, although ETR protein is equally expressed. (B) By zymography, increased size and staining of both pro- and active forms of MMP-9 particularly in ruptured plaques, although MMP-2 activity was not different in each lane as observed in mRNA analysis.

$n=4$) than in non-disrupted plaques (1.11 ± 0.12, $n=6$, $p<0.05$), despite the equal expression of an internal marker protein, endothelin-1 receptor (Fig. 2A). Interestingly, the amount of active form MMP-9 determined by zymography was significantly higher in the disrupted (2.62 ± 0.12) than in non-disrupted plaques (0.72 ± 0.07, $p<0.05$), although pro MMP-9 activity was not significantly different in disrupted (1.8 ± 0.10) and non-disrupted plaques (1.4 ± 0.11) (Fig. 2B). There were no significant differences between the levels of pro and active forms of MMP-2, as demonstrated in its mRNA expression.

3.3. Immunohistochemistry

In the adjacent control regions (Fig. 3A), there was mild atherosclerosis where a few CD-68 positive macrophages existed. Under these conditions, MMPs and TIMPs were scatteringly positive. In contrast, TFPI-2 was diffusely positive in the intima and media. Plaque regions mainly consisted of lipid-rich core and fibrous tissue (Fig. 3B) where CD-68 positive macrophages were accumulated particularly in the shoulder regions of atheroma and all MMPs and TIMPs were strongly positive. It was interesting that, under these conditions, TFPI-2 was regionally positive in the plaque regions. Because of small number of examined plaques, we could not correlate expression of MMPs, TIMPs and TFPI-2 to the stage of plaque development.

4. Discussion

4.1. Gene expression of MMPs, TIMPs and TFPI-2 in plaque

One of the striking findings of the present study was that with a decreased TFPI-2 gene expression, the MMP-9 gene together with the MMP-9 protein was significantly upregulated in plaques, particularly in plaques with disrupted fibrous cap. Increased production of MMP-9 is thought to contribute to the progressive deterioration of the elastic lamellae associated with vessel remodeling, which could be closely related to the occurrence of plaque disruption [15]. Indeed, previous studies indicated that MMP-9 was present in the coronary plaque from unstable angina [16] and carotid plaque from

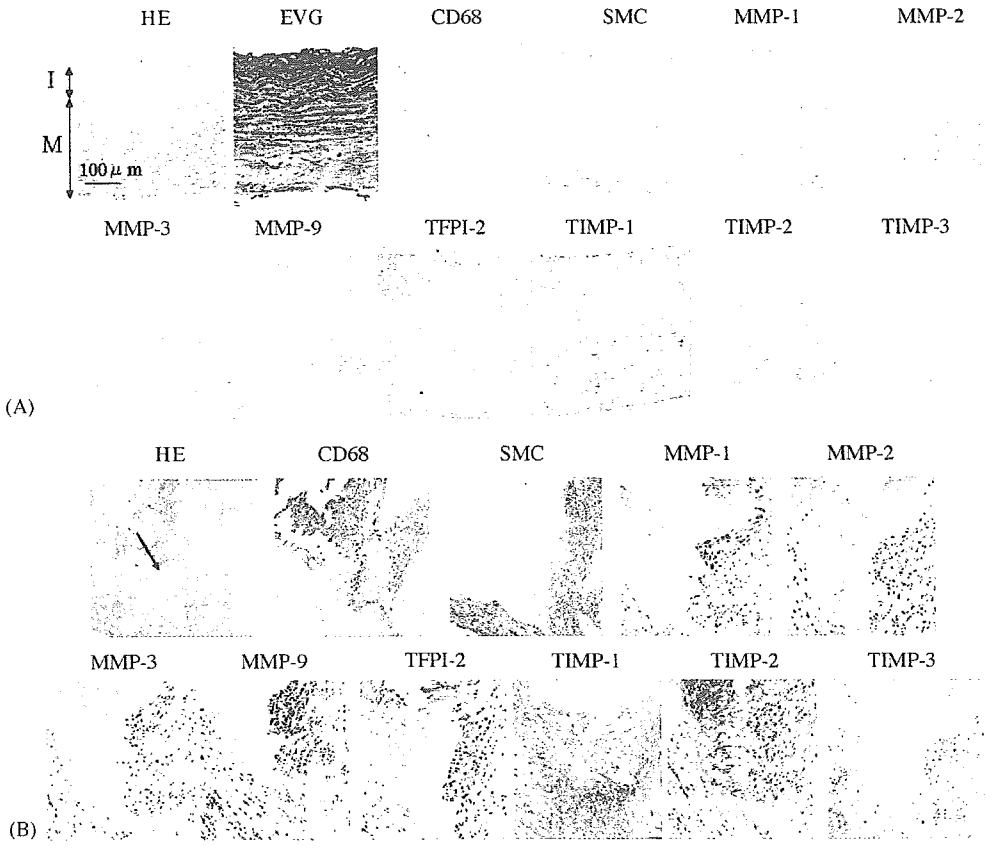

Fig. 3. Histologic and immunohistologic findings (with original magnification of ×25). (A) In the control tissues, there existed mild atherosclerotic lesion where a few CD-68 positive macrophages was found. Under these conditions, tissue factor pathway inhibitor (TFPI)-2 was diffusely positive in the intima and media, although matrix metalloproteinases (MMPs) and tissue inhibitor of MMPs (TIMPs) were scatteringly positive. An arrow indicates boundary between intima and media. (B) In plaque lesions with a lipid-rich core where CD-68 positive macrophages were accumulated, all MMPs and TIMPs were strongly positive particularly in the shoulder regions of atheroma (arrow). It was interesting that, under these conditions, TFPI-2 was regionally positive in this lesion. EVG, elastica van Gieson; HE, hematoxylin–eosin; I, intima; M, media; SMC, smooth muscle cell.

symptomatic patients [17]. We in fact demonstrated greater upregulation and function of MMP-9 in plaques with fissured fibrous cap at the mRNA as well as protein level, based on histological findings.

Simultaneous upregulation of the MMP-1 and -3 genes was also observed, as previously reported [18,19]. MMP-1 specifically cleaves collagen types I and III, which are key components of the extracellular framework of the arterial wall and major constituents of human atherosclerotic plaques, and activate other MMPs [6] that degrade denatured collagen, gelatin and elastin. MMP-3 has the widest substrate repertoire of all MMPs, showing activity against most of the extracellular proteins and proteoglycans [20]. However, unlike MMP-9, there were no differences in the expression of MMP-1 and -3 genes between plaques with and without rupture. This suggests that simultaneous upregulation of these MMPs is a plausible phenomenon in the development of atherosclerotic plaques.

This study demonstrates diminished gene expression of TFPI-2 in plaques that contain abundant MMPs. TFPI-2, originally considered as a serine proteinase inhibitor, is known to be highly expressed in smooth muscle cells of the relatively non-diseased tissue favoring ECM stability by inactivating collagenases such as MMP-1 as well as gelatinases probably through direct protein/protein interactions. Indeed, Herman et al. [7] demonstrate inverse relation between TFPI and MMP activity in atherosclerotic tissue. Thus, decreased TFPI-2 gene expression in plaques, as observed in the present study, might allow increased matrix degradation by MMP-1, -3 and -9 in plaques, enhancing their susceptibility to plaque development. It is interesting, under these conditions, TIMP-1 exhibited significantly higher expression in plaques than in controls. The combined deletion of TIMP-1 and ApoE in mice leads to a reduction in atherosclerotic plaque size [21], whereas overexpression of TIMP-1 induced by adenovirus-mediated transfer in ApoE-deficient mice leads to a decrease in plaque size and an increase in collagen content [22]. Taken together, under the condition where TFPI-2 was diminished to express, upregulation of TIMP-1 seems to counteract overexpression of MMPs, to exert an inhibitory effect on the development of atherosclerotic plaque.

However, the expression ratios of MMPs to TIMP-1 were still higher in the plaque compared with the control regions. Compensatory expression of TIMP-1 might not be sufficient to counteract the degenerative role of MMPs in the plaque, thus contributing to the development of atherosclerotic plaque. Particularly, the MMP-9/TIMP-1 ratio was significantly higher in plaques with disruption than in those without disruption. This suggests the functional significance of the imbalance of expression of these genes in the occurrence of plaque disruption. It would be of interest to examine which can play a more important role, TFPI-2 or TIMP-1, for the regulation of MMP activity, since compartmentalization might result in distinct microenvironments with corresponding variations in MMP/inhibitor ratios.

4.2. Clinical implications and limitations

A recent experimental study in which local MMP-9 was upregulated by gene transfection resulted in enhanced formation of local thrombus [23]. On the contrary, manipulation to augment expression of expression of TIMPs prevented the occurrence of plaque disruption [22]. Therefore, one might speculate that the altered balance of MMP-9/TIMP-1 with decreased TFPI-2 observed in the present study contributes to plaque disruption associated with or without regional thrombosis.

The carotid plaques examined in the present study were obtained from highly stenotic lesion probably representing the final stage of plaque development and destabilization. In acute coronary syndrome, however, atherosclerotic plaque disruption is known to occur at the sites of mild to moderate stenotic lesions [24] that were not examined in the present study. Although preliminary results indicate that in coronary plaques related to acute coronary syndrome MMP-9 gene was highly expressed in comparison with that in plaques from stable coronary disease [25], further study will need to confirm gene expression in carotid plaque from mild to moderate stenotic lesion.

The present study has a limitation regarding histological assessment of the presence of plaque disruption. Only a small portion of each plaque was examined histologically, and it may well be that features were missed in some patients. Several reports suggest that vulnerability to plaque rupture is a multifocal phenomenon particularly at the time of acute presentation [26,27]. Conversely, one might argue that we did not necessarily determine mRNA expression levels in the part of the plaque where histological analysis was performed. Even under these conditions, imbalanced expression of MMPs/TIMPs with reduction of TFPI-2 was observed in plaques, particularly in those associated with disruption. That the control regions were obtained from adjacent to the culprit lesion is another limitation. However, there was no histological evidence for plaque disruption in the control regions used for present study even in the presence of mild atherosclerosis. It can not be excluded, however, that the disruption of the fibrous cap could be resulted from surgical procedure, although we carefully examined the part of plaque where surgical procedures was not affected.

Whether upregulation of MMPs is the cause or result of plaque disarrangement is unclear. A recent study suggested that MMP-9 might have a protective effect against plaque development in double ApoE and MMP-9 knockout mice [28]. Thus, a causal relationship cannot be concluded until a controlled trial with a specific MMP-9 inhibitor is performed. Recently, MMP-8, traditionally associated only with neutrophils, which enhanced matrix breakdown by activating MMPs and/or by inactivating TIMP-1, was found to be highly expressed in macrophages in disrupted plaques [29]. Reduced expression of TFPI-2 might be related to the enhanced expression of neutrophil elastase in plaques, although MMP-

8 gene expression was not determined in the present study.

In the present study, we used real-time RT-PCR, which gives an estimate of mRNA expression instead of protein level for each enzyme and inhibitor, because it is still difficult to extract some proteases such as MMP-1, which binds strongly to connective tissue and to quantitatively assay enzyme activities [30]. However, it is important to determine the activity of TIMPs in protein level, since determination of gene expression can sometimes misinterpret the actual change of protein expression [31]. Therefore, evaluation of mRNA expression of multiple genes by the present real-time RT-PCR method in combination with determination of protein should be done for systematic evaluation of the activities of MMPs, TIMPs and TFPI-2 in clinical tissue samples.

Finally, the precise mechanism of the sustained overexpression of MMPs and TIMPs with reduction of TFPI-2 in advanced atherosclerotic plaque is still unclear. Our preliminarily report indicate that CXCR-2, a chemokine receptor, gene was highly upregulated in accordance with MMP expression in macrophages [32]. This suggests that overexpression of MMPs could be related to a continuous inflammatory reaction, although there was no difference in serum levels of hs-CRP between patients with ruptured and non-ruptured plaques. Further study of the regulatory mechanisms of chemokine and cytokine systems with transcription factors that also play a crucial role in MMP expression [33] may demonstrate a significant pathway for the expression and activation of proteinases and their inhibitors in human atherosclerotic lesions.

5. Conclusion

We applied a real-time RT-PCR method to quantitate mRNA expression in small samples of human carotid plaque. Levels of MMP-1, -3, -9 and TIMP-1 mRNAs were significantly upregulated in human carotid plaque where TFPI-2 mRNA was decreased to be expressed. The particular upregulation of MMP-9 and resultant imbalance of MMP-9/TIMP-1 expression could play a pivotal role in plaque disruption.

Acknowledgements

This work was supported in part by grants from the Ministry of Health, Welfare and Labor of Japan and from the Cardiovascular Research Foundation (to M.Y.), the Promotion of Fundamental Studies in Health Science of the Organization for Pharmaceutical Safety and Research (OPSR) of Japan (to A.S.), and the Japan Cardiovascular Research Foundation (to A.S.). A part of this work was presented at the 53rd Annual Scientific Session, American College of Cardiology, in New Orleans, 2004.

References

[1] Falk E, Shah PK, Fuster V. Coronary plaque disruption. Circulation 1995;92:657–71.
[2] Carr S, Farb A, Pearce WH, et al. Atherosclerotic plaque rupture in symptomatic carotid artery stenosis. J Vasc Surg 1996;23:755–65.
[3] Libby P. Inflammation in atherosclerosis. Nature 2002;420:868–74.
[4] Dollery CM, McEwan JR, Henney AM. Matrix metalloproteinases and cardiovascular disease. Circ Res 1995;77:863–8.
[5] Galis ZS, Khatri JJ. Matrix metalloproteinases in vascular remodeling and atherogenesis: the good, the bad, and the ugly. Circ Res 2002;90:251–62.
[6] Nagase H. Activation mechanisms of matrix metalloproteinases. Biol Chem 1997;378:151–60.
[7] Herman MP, Sukhova GK, Kisiel W, et al. Tissue factor pathway inhibitor-2 is a novel inhibitor of matrix metalloproteinases with implications for atherosclerosis. J Clin Invest 2001;107:1117–26.
[8] Fabunmi RP, Sukhova GK, Sugiyama S, et al. Expression of tissue inhibitor of metalloproteinases-3 in human atheroma and regulation in lesion-associated cells: a potential protective mechanism in plaque stability. Circ Res 1998;83:270–8.
[9] Galis ZS, Sukhova GK, Lark MW, et al. Increased expression of matrix metalloproteinases and matrix degrading activity in vulnerable regions of human atherosclerotic plaques. J Clin Invest 1994;94:2493–503.
[10] Brew K, Dinakarpandian D, Nagase H. Tissue inhibitors of metalloproteinases: evolution, structure and function. Biochim Biophys Acta 2000;1477:267–83.
[11] Knox JB, Sukhova GK, Whittemore AD, et al. Evidence for altered balance between matrix metalloproteinases and their inhibitors in human aortic diseases. Circulation 1997;95:205–12.
[12] Sternlicht MD, Werb Z. How matrix metalloproteinases regulate cell behavior. Annu Rev Cell Dev Biol 2001;17:463–516.
[13] Higashikata T, Yamagishi M, Sasaki H, et al. Application of real-time RT-PCR to quantifying gene expression of matrix metalloproteinases and tissue inhibitors of metalloproteinases in human abdominal aortic aneurysm. Atherosclerosis 2004;177:353–60.
[14] Kolodgie FD, Burke AP, Farb A, et al. The thin-cap fibroatheroma: a type of vulnerable plaque, the major precursor lesion to acute coronary syndrome. Curr Opin Cardiol 2001;16:285–92.
[15] Schoenhagen P, Ziada KM, Kapadia SR, et al. Extent and direction of arterial remodeling in stable versus unstable coronary syndromes: an intravascular ultrasound study. Circulation 2000;101:598–603.
[16] Brwon DL, Hibbs MS, Kearney M, et al. Identification of 92-kD gelatinase in human coronary atherosclerotic lesions. Association of active enzyme synthesis with unstable angina. Circulation 1995;91:2125–31.
[17] Loftus IM, Naylor AR, Goodall S, et al. Increased matrix metalloproteinase-9 activity in unstable carotid plaques. A potential role in acute plaque disruption. Stroke 2000;31:40–7.
[18] Nikkari ST, O'Brien KD, Ferguson M, et al. Intestinal collagenase (MMP-1) expression in human carotid atherosclerosis. Circulation 1995;92:1393–8.
[19] Sukhova GK, Schonbeck U, Rabkin E, et al. Evidence for increased collagenolysis by intersitial collagenases-1 and -3 in vulnerable atheromatous plaques. Circulation 1999;99:2503–9.
[20] Sato H, Takino T, Okada Y, et al. A matrix metalloproteinase expressed on the surface of invasive tumor cells. Nature 1994;370:61–5.
[21] Silence J, Collen D, Lijnen HR. Reduced atherosclerotic plaque but enhanced aneurysm formation in mice with inactivation of the tissue inhibitor of metalloproteinase-1 (TIMP-1) gene. Circ Res 2002;90:897–903.
[22] Rouis M, Adamy C, Duverger N, et al. Adenovirus-mediated overexpression of tissue inhibitor of metalloproteinase-1 reduces atherosclerotic lesions in apolipoprotein E-deficient mice. Circulation 1999;100:533–40.

[23] Morishige K, Shimokawa H, Matsumoto Y, et al. Overexpression of matrix metalloproteinase-9 promotes intravascular thrombus formation in porcine coronary arteries in vivo. Cardiovasc Res 2003;57:572–85.
[24] Yamagishi M, Terashima M, Awano K, et al. Morphology of vulnerable coronary plaque: insights from follow-up of patients examined by intravascular ultrasound before an acute coronary syndrome. J Am Coll Cardiol 2000;35:106–11.
[25] Higo S, Nanto S, Higashikata T, et al. Impact of altered expression balance of matrix metalloproteinases and tissue inhibitor of metalloproteinases genes on coronary plaque rupture: results from quantitative tissue analysis using real-time reverse transcriptase-polymerase chain reaction method (abstr). J Am Coll Cardiol 2004;43(Suppl. A):257A.
[26] Rioufol G, Finet G, Ginon I, et al. Multiple atherosclerotic plaque rupture in acute coronary syndrome. A three-vessel intravascular ultrasound study. Circulation 2002;106:804–8.
[27] Schoenhagen P, Stone GW, Nissen SE, et al. Coronary plaque morphology and frequency of ulceration distant from culprit lesions in patients with unstable and stable presentation. Arterioscler Thromb Vasc Biol 2003;23:1895–900.
[28] Johnson J, George A, Newby C. Matrix metalloproteinase-9 and -12 have opposite effects on atherosclerotic plaque stability (abstr). Atherosclerosis 2003;4(Suppl.):196.
[29] Dollery CM, Owen CA, Sukhova GK, et al. Neutrophil elastase in human atherosclerotic plaques. Production by macrophages. Circulation 2003;107:2829–36.
[30] Woessner JR. Quantification of matrix metalloproteinases in tissue samples. Methods Enzymol 1995;248:510–28.
[31] Blindt R, Vogt F, Lamby D, et al. Characterization of differential gene expression in quiescent and invasive human arterial smooth muscle cells. J Vasc Res 2002;39:340–52.
[32] Yamagishi M, Higashikata T, Higashi T, et al. Sustained upregulation of chemokine and its receptor genes associated with matrix metalloproteinase overexpression in human carotid plaque rupture: results from a quantitative study with real-time reverse transcriptase-polymerase chain reaction method (abstr). J Am Coll Cardiol 2004;43(Suppl.):497A.
[33] Chase AJ, Bond M, Crook MF, et al. Role of nuclear NF-κB activation in metalloproteinase-1 -3 and -9 secretion by human macrophages in vitro and rabbit form cells produced in vivo. Arterioscler Thromb Vasc Biol 2002;22:765–71.

Transplantation of Mesenchymal Stem Cells Improves Cardiac Function in a Rat Model of Dilated Cardiomyopathy

Noritoshi Nagaya, MD; Kenji Kangawa, PhD; Takefumi Itoh, MD; Takashi Iwase, MD; Shinsuke Murakami, MD; Yoshinori Miyahara, MD; Takafumi Fujii, MD; Masaaki Uematsu, MD; Hajime Ohgushi, MD; Masakazu Yamagishi, MD; Takeshi Tokudome, MD; Hidezo Mori, MD; Kunio Miyatake, MD; Soichiro Kitamura, MD

Background—Pluripotent mesenchymal stem cells (MSCs) differentiate into a variety of cells, including cardiomyocytes and vascular endothelial cells. However, little information is available about the therapeutic potency of MSC transplantation in cases of dilated cardiomyopathy (DCM), an important cause of heart failure.

Methods and Results—We investigated whether transplanted MSCs induce myogenesis and angiogenesis and improve cardiac function in a rat model of DCM. MSCs were isolated from bone marrow aspirates of isogenic adult rats and expanded ex vivo. Cultured MSCs secreted large amounts of the angiogenic, antiapoptotic, and mitogenic factors vascular endothelial growth factor, hepatocyte growth factor, adrenomedullin, and insulin-like growth factor-1. Five weeks after immunization, MSCs or vehicle was injected into the myocardium. Some engrafted MSCs were positive for the cardiac markers desmin, cardiac troponin T, and connexin-43, whereas others formed vascular structures and were positive for von Willebrand factor or smooth muscle actin. Compared with vehicle injection, MSC transplantation significantly increased capillary density and decreased the collagen volume fraction in the myocardium, resulting in decreased left ventricular end-diastolic pressure (11 ± 1 versus 16 ± 1 mm Hg, $P<0.05$) and increased left ventricular maximum dP/dt (6767 ± 323 versus 5138 ± 280 mm Hg/s, $P<0.05$).

Conclusions—MSC transplantation improved cardiac function in a rat model of DCM, possibly through induction of myogenesis and angiogenesis, as well as by inhibition of myocardial fibrosis. The beneficial effects of MSCs might be mediated not only by their differentiation into cardiomyocytes and vascular cells but also by their ability to supply large amounts of angiogenic, antiapoptotic, and mitogenic factors. (***Circulation.*** **2005;112:1128-1135.)**

Key Words: myocytes ■ angiogenesis ■ heart failure ■ growth substances ■ transplantation

Despite advances in medical and surgical procedures, congestive heart failure remains a leading cause of cardiovascular morbidity and mortality.[1] Idiopathic dilated cardiomyopathy (DCM), a primary myocardial disease of unknown etiology characterized by a loss of cardiomyocytes and an increase in fibroblasts, is an important cause of heart failure.[2] Although myocyte mitosis and the presence of cardiac precursor cells in adult hearts have recently been reported,[3] the death of large numbers of cardiomyocytes results in the development of heart failure. Thus, restoring lost myocardium would be desirable for the treatment of DCM.

Mesenchymal stem cells (MSCs) are pluripotent, adult stem cells residing within the bone marrow microenvironment.[4] In contrast to their hematopoietic counterparts, MSCs are adherent and can be expanded in culture. MSCs can differentiate not only into osteoblasts, chondrocytes, neurons, and skeletal muscle cells but also into vascular endothelial cells[5] and cardiomyocytes.[6,7] In vitro, MSCs can be induced to differentiate into beating cardiomyocytes by 5-azacytidine treatment.[8] In vivo, MSCs directly injected into an infarcted heart have been shown to induce myocardial regeneration and improve cardiac function.[9] In addition, MSC implantation induces therapeutic angiogenesis in a rat model of hindlimb ischemia through vascular endothelial growth factor (VEGF) production by MSCs.[10,11] Myocardial blood flow abnormalities, even in the presence of angiographically normal coronary arteries, have been documented in patients with DCM.[12]

Received August 18, 2004; revision received April 28, 2005; accepted May 10, 2005.

From the Departments of Regenerative Medicine and Tissue Engineering (N.N., T.I., T.I., S.M.), Internal Medicine (N.N., M.Y., K.M.), Biochemistry (K.K., T.T.), and Cardiac Physiology (Y.M., T.F., H.M.), National Cardiovascular Center Research Institute, Osaka; the Cardiovascular Division (M.U.), Kansai Rosai Hospital, Hyogo; the Tissue Engineering Research Center (H.O.), National Institute of Advanced Industrial Science and Technology, Hyogo; and the Department of Cardiovascular Surgery (S.K.), National Cardiovascular Center, Osaka, Japan.

Reprint requests to Noritoshi Nagaya, MD, Department of Regenerative Medicine and Tissue Engineering, National Cardiovascular Center Research Institute, 5-7-1 Fujishirodai, Suita, Osaka 565-8565, Japan. E-mail nnagaya@ri.ncvc.go.jp

Circulation **is available at http://www.circulationaha.org** **DOI: 10.1161/CIRCULATIONAHA.104.500447**

These findings raise the possibility that transplanted MSCs have beneficial effects on myocardial structure and function via myogenesis and angiogenesis. However, little information is available about the therapeutic potential of MSCs for DCM.

A unique model of myocarditis in the rat has been created by immunization with porcine cardiac myosin,[13] which results in severe heart failure characterized by increased cardiac fibrosis and left ventricular (LV) dilation.[14] Thus, the late phase of this model can serve as a model of DCM.

The purpose of this study was to investigate the following topics: (1) whether transplantation of MSCs induces myogenesis and angiogenesis, decreases collagen deposition in the myocardium, and thereby improves cardiac function in a rat model of DCM and (2) whether the beneficial effects of MSCs are mediated by their differentiation into cardiomyocytes and vascular cells and/or by their supplying angiogenic, antiapoptotic, and mitogenic factors.

Methods

Expansion of Bone Marrow MSCs

MSC expansion was performed according to previously described methods.[4] In brief, we humanely killed male Lewis rats and harvested bone marrow by flushing their femoral and tibial cavities with phosphate-buffered saline (PBS). Bone marrow cells were cultured in α-minimal essential medium supplemented with 10% fetal bovine serum and antibiotics. A small number of cells developed visible symmetric colonies by days 5 to 7. Nonadherent hematopoietic cells were removed, and the medium was replaced. The adherent, spindle-shaped MSC population expanded to $>5\times10^7$ cells within $\approx$4 to 5 passages after the cells were first plated.

Flow Cytometry

Cultured MSCs were analyzed by fluorescence-activated cell sorting (FACS) (FACScan flow cytometer, Becton Dickinson). Cells were incubated with fluorescein isothiocyanate (FITC)–conjugated mouse monoclonal antibodies against rat CD31 (clone TLD-3A12, Becton Dickinson), CD34 (clone ICO-115, Santa Cruz), CD45 (clone OX-1, Becton Dickinson), CD90 (clone OX-7, Becton Dickinson), vimentin (clone V9, Dako), and smooth muscle actin (SMA; clone 1A4, Dako). FITC-conjugated hamster anti-rat CD29 monoclonal antibody (clone Ha2/5, Becton Dickinson) and rabbit anti-rat c-Kit polyclonal antibody (clone C-19, Santa Cruz) were used. Isotype-identical antibodies served as controls.

Model of DCM

Male Lewis rats weighing 220 to 250 g (Japan SLC Inc, Hamamatsu, Japan) were used in this study. These isogenic rats served as donors and recipients of MSCs to simulate autologous implantation. DCM was produced by inducing experimental myocarditis, as described previously.[13,14] In brief, 1 mg (0.1 mL) of porcine heart myosin (Sigma) was mixed with an equal volume of Freund's complete adjuvant (Sigma) and injected into a footpad on days 1 and 7. Five weeks after immunization, these rats served as a model of heart failure due to DCM.

MSC Transplantation

In a preliminary experiment, we performed dose-response studies to obtain the maximal effects of cell transplantation. Because the effect of 10^6 MSCs was modest, we used 5×10^6 MSCs for transplantation. Five weeks after immunization, we injected a total of 5×10^6 MSCs/100 μL PBS, or PBS alone, into the myocardium at 10 points. In brief, the LV was divided into 3 levels (basal, middle, and apical). The basal and middle levels were each subdivided into 4 segments, and the apical level was subdivided into 2 segments. Injection into each segment was performed with a 27-gauge needle. Sham rats received intramyocardial injections of 100 μL PBS. This protocol resulted in the creation of 3 groups: DCM rats given MSCs (MSC-treated DCM group, n=10); DCM rats given PBS (untreated DCM group, n=10); and sham rats given PBS (sham group, n=10). The Animal Care Committee of the National Cardiovascular Center approved this experimental protocol.

Echocardiographic Studies

Echocardiographic studies were performed by an investigator, blinded to treatment allocation, at 5 weeks after immunization (before treatment) and 4 weeks after cell transplantation (after treatment). Two-dimensional, targeted M-mode tracings were obtained at the level of the papillary muscles with an echocardiographic system equipped with a 7.5-MHz transducer (HP Sonos 5500, Hewlett-Packard).[15] LV dimensions were measured according to the American Society for Echocardiology leading-edge method from at least 3 consecutive cardiac cycles. Fractional shortening was calculated as (LVDd−LVDs)/LVDd×100, where LVDd=LV diastolic dimension and LVDs=LV systolic dimension.

Hemodynamic Studies

Hemodynamic studies were performed 4 weeks after cell transplantation. A 1.5F micromanometer-tipped catheter (Millar Instruments) was inserted into the right carotid artery for measurement of mean arterial pressure.[16] Next, the catheter was advanced into the LV for measurement of LV pressure. Hemodynamic variables were measured with a pressure transducer (model P23 ID, Gould) connected to a polygraph. After completion of these measurements, the left and right ventricles were excised and weighed.

Histological Examination

To detect fibrosis in cardiac muscle, the LV myocardium (n=5 from each group) was fixed in 10% formalin, cut transversely, embedded in paraffin, and stained with Masson's trichrome. Transverse sections were randomly obtained from the 3 levels (basal, middle, and apical), and 20 randomly selected fields per section (n=60 per animal) were analyzed. After each field was scanned and computerized with a digital image analyzer (WinRoof, Mitani Co), collagen volume fraction was calculated as the sum of all areas containing connective tissue divided by the total area of the image.[15]

To detect capillaries in the myocardium, samples of harvested muscle (n=5 each) were embedded in OCT compound (Miles Scientific), snap-frozen in LN_2, cut into transverse sections, and stained for alkaline phosphatase by an indoxyltetrazolium method. Transverse sections were randomly obtained from the 3 levels (basal, middle, and apical), and 5 randomly selected fields per section (n=15 per animal) were analyzed. The number of capillaries was counted by light microscopy at a magnification of ×200. The number of capillaries in each field was averaged and expressed as the number of capillary vessels. These morphometric studies were performed by 2 examiners who were blinded to treatment assignment.

Assessment of Cell Differentiation

Suspended MSCs were labeled with fluorescent dyes with use of a PKH26 red fluorescent cell linker kit (Sigma), as reported previously.[17] Fluorescence-labeled MSCs were injected into the myocardium 5 weeks after immunization. Rats (n=5) were humanely killed 4 weeks after cell transplantation. LV samples were embedded in OCT compound, snap-frozen in LN_2, and cut into sections. Immunofluorescence staining was performed with monoclonal mouse anti-cardiac troponin T (Novo), anti-desmin (Dako), anti-connexin-43 (Sigma), polyclonal rabbit anti–von Willebrand factor (Dako), and monoclonal mouse SMA (Dako). FITC-conjugated IgG antibody (BD Pharmingen) was used as a secondary antibody. To perform quantitative analysis of the magnitude of MSC differentiation into cardiomyocytes, heart cells from each rat (n=5) were isolated by incubation in balanced salt solution containing 0.06% collagenase type II (Worthington Biochemical Co), as reported previously.[18] PKH26/troponin T double-positive cells were detected by FACS.

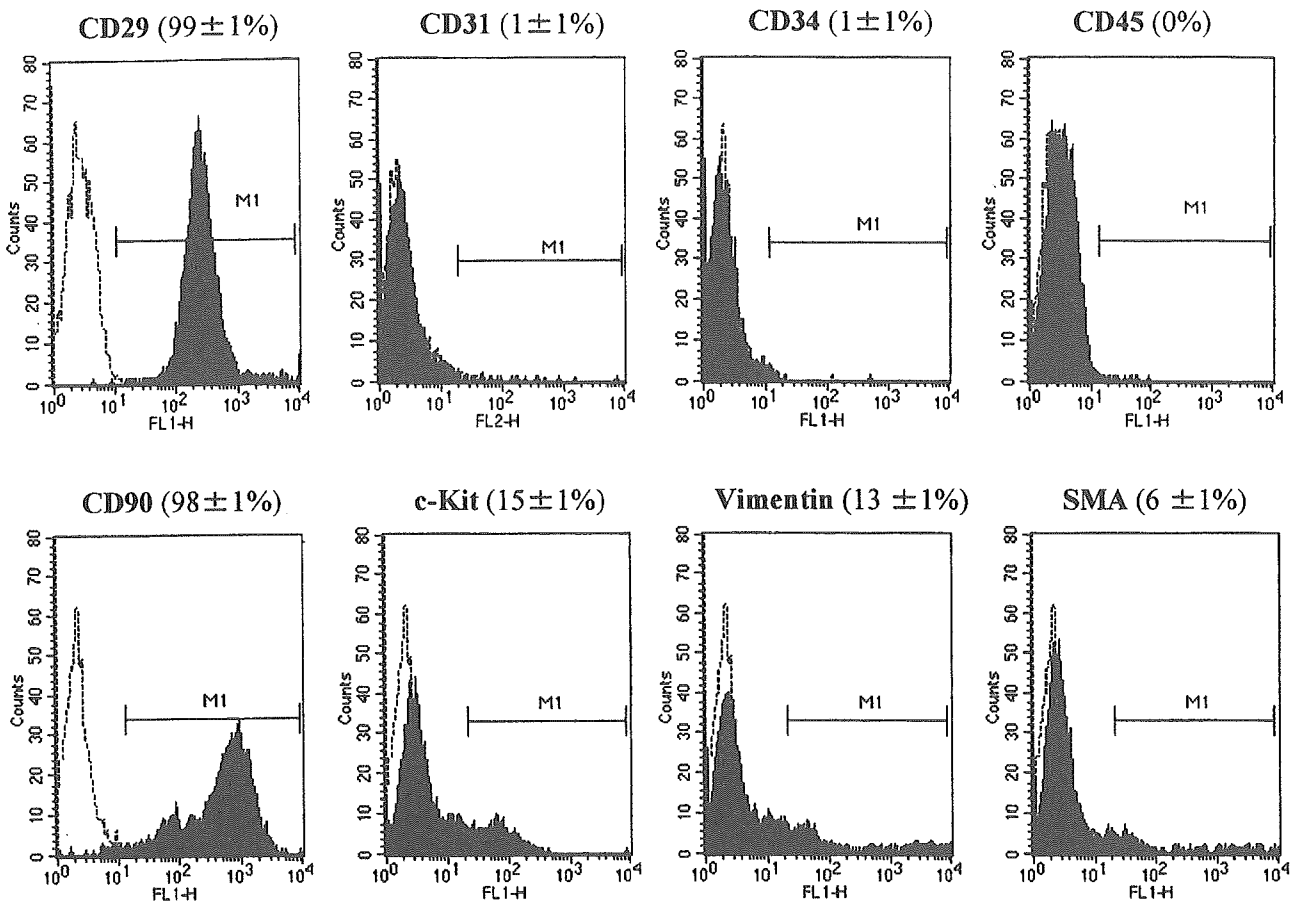

Figure 1. Flow-cytometric analysis of the adherent, spindle-shaped MSC population expanded to 4 to 5 passages. Most of the MSCs expressed CD29 and CD90, whereas they were negative for CD31, CD34, CD45, and SMA. Some of the cells were positive for c-Kit and vimentin.

Western Blot Analysis of Matrix Metalloproteinases

To identify the protein expression of matrix metalloproteinases (MMPs)-2 and -9, Western blotting was performed with rabbit polyclonal antibody raised against MMP-2 (Laboratory vision Co) and MMP-9 (Chemicon Co). The LV obtained from individual rats was used for comparison among the 3 groups (n=5 each). These samples were homogenized on ice in 0.1% Tween 20 homogenization buffer with a protease inhibitor. Then, 40 μg of protein was transferred into sample buffer, loaded on a 7.5% sodium dodecyl sulfate–polyacrylamide gel, and blotted onto a polyvinylidene fluoride membrane (Millipore Co). After being blocked for 120 minutes, the membrane was incubated with primary antibody at a dilution of 1:200. The membrane was incubated with peroxidase labeled with secondary antibody at a dilution of 1:1000. Positive protein bands were visualized with an ECL kit (Amersham) and measured by densitometry. Western blot analysis with a mouse polyclonal antibody raised against β-actin (Santa Cruz) was used as a protein loading control.

Assay for Angiogenic, Antiapoptotic, and Mitogenic Factors

To investigate whether MSCs produce angiogenic and growth factors, we measured VEGF, hepatocyte growth factor (HGF), insulin-like growth factor-1 (IGF-1), and adrenomedullin (AM) levels in conditioned medium 24 hours after medium replacement. VEGF, HGF, and IGF-1 were measured by enzyme immunoassay (VEGF immunoassay, R&D Systems Inc; rat HGF enzyme immunoassay, Institute of Immunology Co, Ltd; and active rat IGF-1 enzyme immunoassay, Diagnostic Systems Laboratories, Inc). AM level was measured with a radioimmunoassay kit (Shionogi Co), as reported previously.[19] The amounts of these products produced by MSCs were compared with those produced by bone marrow–derived mononuclear cells (MNCs) because MNCs have commonly been used for regenerative therapy.[19–21] There was no significant difference in cell viability between MSCs and MNCs 24 hours after seeding (88±5% versus 85±4% by trypan blue solution). In vivo, circulating levels of VEGF, HGF, IGF-1, and AM were measured before and 24 hours after administration of MSCs or vehicle (n=6 from each group).

Statistical Analysis

Numerical values are expressed as mean±SEM unless otherwise indicated. Comparisons of parameters between 2 groups were made with unpaired Student t test. Comparisons of parameters among 3 groups were made with a 1-way ANOVA, followed by the Scheffe multiple-comparison test. Comparisons of changes in parameters among the 3 groups were made by a 2-way ANOVA for repeated measures, followed by the Scheffe multiple-comparison test. A value of $P<0.05$ was considered significant.

Results

Characterization of Cultured MSCs

Most cultured MSCs expressed CD29 and CD90 (Figure 1). In contrast, the majority of MSCs were negative for CD31, CD34, CD45, and SMA. Some of the MSCs expressed c-Kit and vimentin.

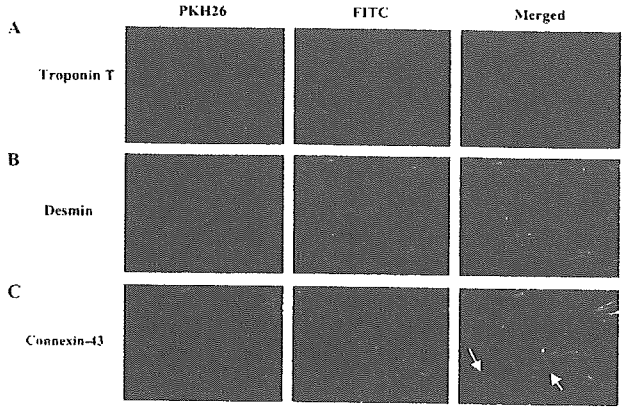

Figure 2. Differentiation of transplanted MSCs into cardiomyocytes. Transplanted MSCs were engrafted in the myocardium and stained for cardiac troponin T (A) and desmin (B). Engrafted MSCs also expressed connexin-43, a gap junction protein, at contact points with native cardiac myocytes (left arrow) and other transplanted cells (right arrow) (C). Magnification ×400.

Myogenesis and Angiogenesis Induced by MSCs

Red fluorescence–labeled MSCs were transplanted into the myocardium 5 weeks after immunization. Four weeks after transplantation, MSCs were engrafted into the myocardium (Figure 2). Immunofluorescence demonstrated that transplanted MSCs were positive for the cardiac markers cardiac troponin T and desmin (Figure 2). Transplanted MSCs also expressed connexin-43, a gap junction protein, at contact points with native cardiac myocytes as well as with MSCs. FACS analysis of isolated heart cells demonstrated that 8±1% of transplanted MSCs were double-positive for PKH26 and troponin T. These results suggest that a small number of transplanted MSCs can differentiate into cardiomyocytes.

Some transplanted MSCs formed vascular structures in the myocardium and were positive for von Willebrand factor (Figure 3A). Other MSCs were positive for SMA and participated in vessel formation as mural cells (Figure 3B). Alkaline phosphatase staining of the ischemic myocardium showed marked augmentation of neovascularization in the MSC-treated DCM group (Figures 4A–4C). Quantitative analysis demonstrated that capillary density was significantly

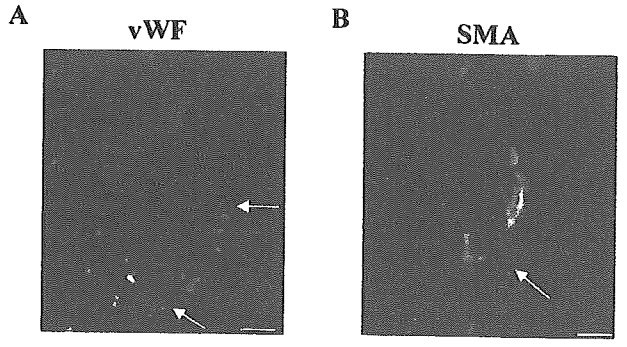

Figure 3. Differentiation of transplanted MSCs into vascular endothelial cells and smooth muscle cells. Some of the transplanted MSCs were positive for von Willebrand factor (vWF, A) and SMA (B) and formed vascular structures (A and B). Scale bars=10 μm.

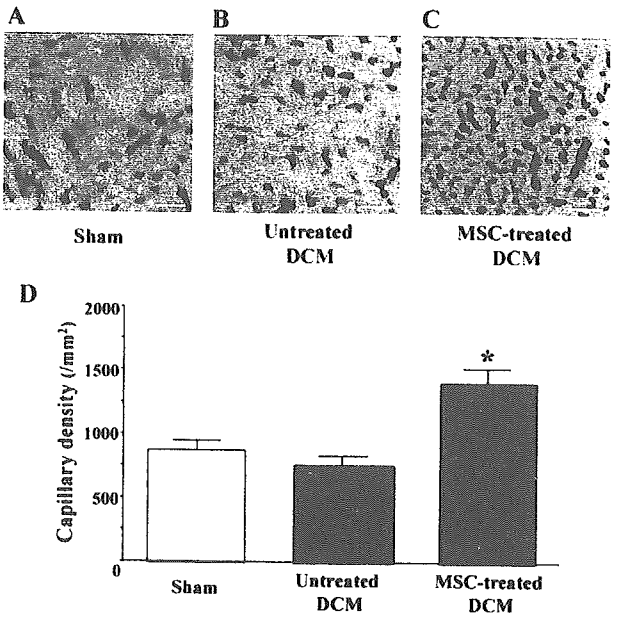

Figure 4. A–C, Representative samples of alkaline phosphatase staining of myocardium. Magnification, ×200. Scale bars=10 μm. D, Quantitative analysis of capillary density in the myocardium. Data are mean±SEM *$P<0.05$ vs untreated DCM group.

higher in the MSC-treated DCM group than in the untreated DCM group (Figure 4D).

Angiogenic, Antiapoptotic, and Mitogenic Factors Released From MSCs

After 24 hours of culture, MSCs secreted large amounts of angiogenic and antiapoptotic factors, including VEGF, HGF, and AM (Figure 5). Compared with MNCs that have commonly been used for regenerative therapy,[20–22] MSCs secreted 4-fold more VEGF and 5-fold more HGF. Similarly, MSCs secreted 6-fold more AM, an angiogenic and antiapoptotic peptide, compared with MNCs. MSCs also secreted a large amount, 10-fold greater than MNCs, of IGF-1, a growth hormone mediator for myocardial growth (Figure 5). Transplantation of MSCs significantly increased circulating VEGF (45.8±1.6 to 68.5±3.6 pg/mL, $P<0.05$), HGF (431.8±56.6 to 517.2±67.1 pg/mL, $P<0.05$), and AM (23.4±0.8 to 41.2±4.8 pg/mL, $P<0.05$) 24 hours after transplantation, although vehicle injection did not alter these parameters. Serum IGF-1 tended to increase after MSC transplantation (938.1±151.6 to 1063.5±116.9 pg/mL, P=NS), but this increase did not reach statistical significance.

Hemodynamic Effects of MSC Transplantation

Nine weeks after immunization, LV end-diastolic pressure showed a marked elevation in the untreated DCM group; this elevation was significantly attenuated in the MSC-treated DCM group (Figure 6A). LV maximum *dP/dt* was significantly lower in the untreated DCM group than in the sham group (Figure 6B). However, LV maximum *dP/dt* was significantly improved 4 weeks after MSC transplantation. There was no significant difference in heart rate or mean arterial pressure among the 3 groups (the Table). Echocardiographic studies demonstrated LV dysfunction and dilation

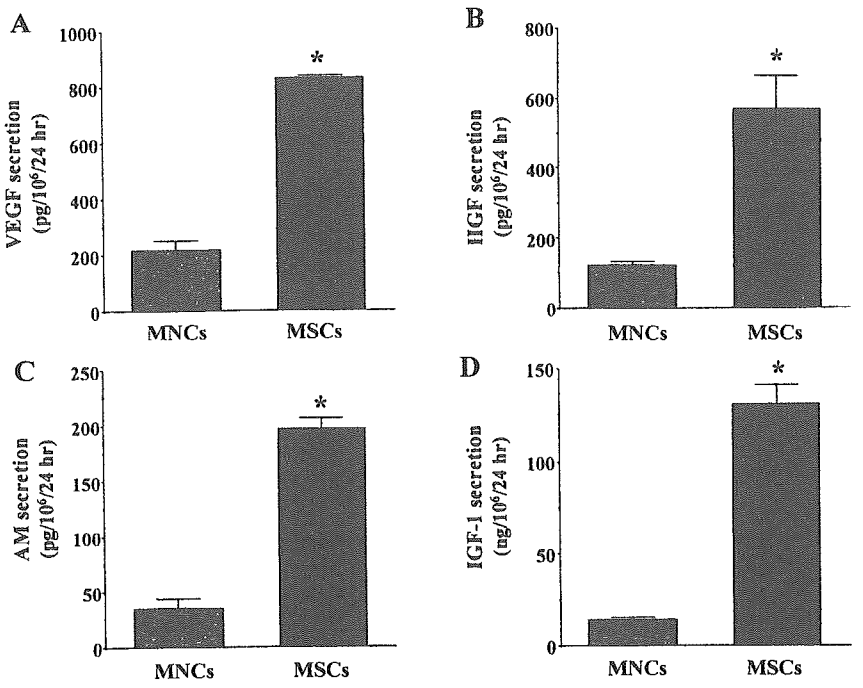

Figure 5. A–D, Angiogenic, antiapoptotic, and mitogenic factors produced by MSCs and bone marrow–derived MNCs). Compared with MNCs, MSCs secreted large amounts of VEGF, HGF, AM, and IGF-1. *$P<0.05$ vs MNCs.

in the untreated DCM group, as indicated by a decrease in percent fractional shortening and an increase in LV diastolic dimension (Figure 6C and 6D). However, MSC transplantation increased percent fractional shortening and inhibited the increase in LV diastolic dimension.

Reduction of Myocardial Fibrosis by MSC Transplantation

Masson's trichrome staining demonstrated modest myocardial fibrosis in the untreated DCM group (Figure 7A). However, MSC transplantation significantly attenuated the development of myocardial fibrosis. Quantitative analysis also demonstrated that the collagen volume fraction in the MSC-treated DCM group was significantly smaller than that in the untreated DCM group (Figure 7B). Western blot analysis showed that myocardial contents of MMP-2 and MMP-9 in the untreated DCM were significantly increased compared with those in the sham group (Figure 7C–E). However, the increases in MMP-2 and MMP-9 levels were attenuated by MSC transplantation, although the change in MMP-9 did not reach statistical significance.

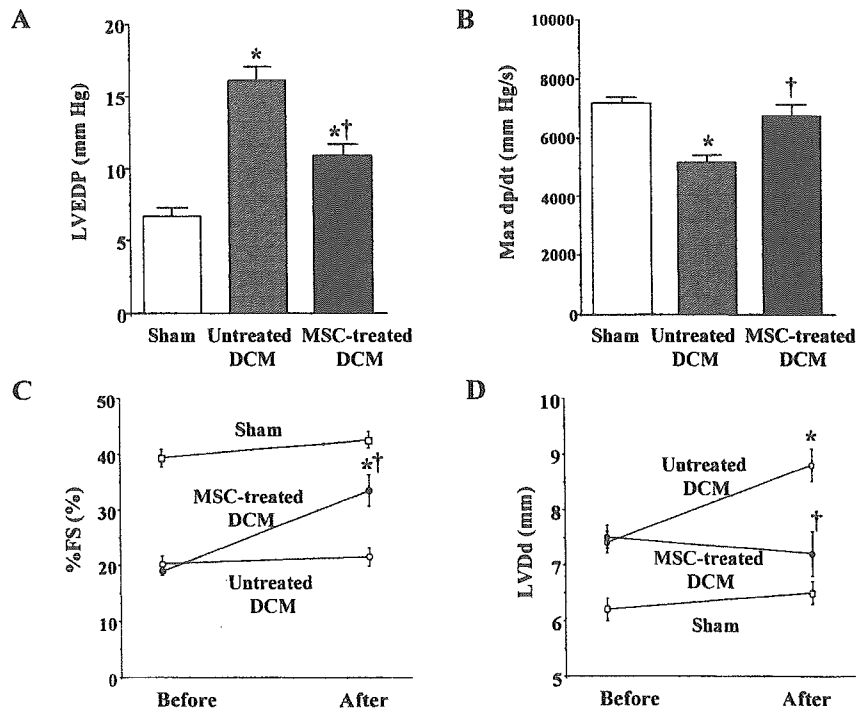

Figure 6. A and B, Effects of MSC transplantation on hemodynamic parameters. LVEDP indicates LV end-diastolic pressure; Max *dP/dt*, LV maximum *dP/dt*. Data are mean±SEM. *$P<0.05$ vs sham group; †$P<0.05$ vs untreated DCM group. C and D, Changes in echocardiographic parameters induced by MSC transplantation. %FS indicates LV fractional shortening. Data are mean±SEM *$P<0.05$ vs before transplantation; †$P<0.05$ vs the time-matched untreated DCM group.

Physiological Profiles of the 3 Experimental Groups

	Sham	Untreated DCM	MSC-Treated DCM
n	10	10	10
Body wt, g	421±8	372±4*	389±5*
LV wt/body wt, g/kg	1.91±0.05	2.18±0.06*	2.05±0.05
RV wt/body wt, g/kg	0.55±0.01	0.68±0.02*	0.60±0.03†
Heart rate, bpm	403±10	432±15	417±12
Mean arterial pressure, mm Hg	134±2	123±3	132±5

wt indicates weight; RV, right ventricle. Sham-operated rats were given vehicle only. The untreated DCM group included DCM rats treated with vehicle. The MSC-treated DCM group included DCM rats treated with MSCs. Data are mean±SEM.

*$P<0.05$ vs sham group; †$P<0.05$ vs untreated DCM group.

Discussion

In the present study, we have demonstrated the following effects of MSC transplantation in a rat model of DCM: (1) induction of myogenesis and angiogenesis; (2) differentiation of transplanted MSCs into cardiomyocytes, vascular endothelial cells, and smooth muscle cells; (3) secretion of large amounts of VEGF, HGF, AM, and IGF-1; (4) improvement of cardiac function and inhibition of ventricular remodeling; and (5) decrease in collagen volume fraction in the myocardium.

Earlier studies have shown that transplantation of MSCs improves cardiac function in experimental models of ischemic heart disease.[9,23] However, little information is available about the therapeutic potential of MSCs for chronic heart failure due to DCM. Previous studies have shown that porcine cardiac myosin-induced myocarditis progresses to a chronic phase resembling DCM.[13,14] Thus, we used this model 5 weeks after immunization as an example of experimental DCM.

In the present study, transplanted MSCs were engrafted into the myocardium in a rat model of DCM. Four weeks after transplantation, some of the engrafted MSCs were positively stained for cardiac troponin T and desmin. Transplanted MSCs also expressed connexin-43, a gap junction protein, at contact points with native cardiac myocytes as well as with MSCs. These results suggest that MSCs differentiate into cardiomyocytes in the myocardium and form connections with native cardiomyocytes in rats with DCM. Unlike earlier studies that have used a model of myocardial infarction,[7,9,23] we used a rat model of DCM to demonstrate the engraftment and cardiogenic differentiation of MSCs. Importantly, MSC transplantation improved cardiac function in these rats, as indicated by a significant decrease in LV end-diastolic pressure and an increase in LV dP/dt_{max}. Thus, the improvement in cardiac function may be a result of MSC-induced myocardial regeneration; however, further studies are necessary to investigate the mechanisms by which MSCs develop into cardiac myocyte–like cells.

Some of the transplanted MSCs were positive for a vascular endothelial cell marker and participated in vessel formation. MSC transplantation significantly increased capillary density in the myocardium. SMA staining revealed that MSCs differentiated into vascular smooth muscle cells, which play an important role in vessel maturation. Earlier studies have shown that transplantation of MNCs induces therapeutic angiogenesis in patients with limb ischemia or ischemic heart disease.[20–22] The angiogenic potential of MNCs is mediated at least in part by production by the cells of a variety of angiogenic factors.[24] Although MSCs have also been shown to produce VEGF,[10,25] there has been no study to compare their production between MSCs and MNCs. The present study demonstrated that MSCs secreted ≈4-fold more VEGF compared with MNCs. Furthermore, MSCs secreted large amounts of HGF and AM, potent angiogenic factors.[26–30] Taking these findings together, MSCs may contribute to neovascularization in the myocardium not only through their ability to generate capillary-like structures but also through growth factor–mediated paracrine regulation. Myocardial blood flow abnormalities have been documented in patients with heart failure caused by DCM.[12] Thus, it is possible that MSC-induced neovascularization contributes to improvement in cardiac function.

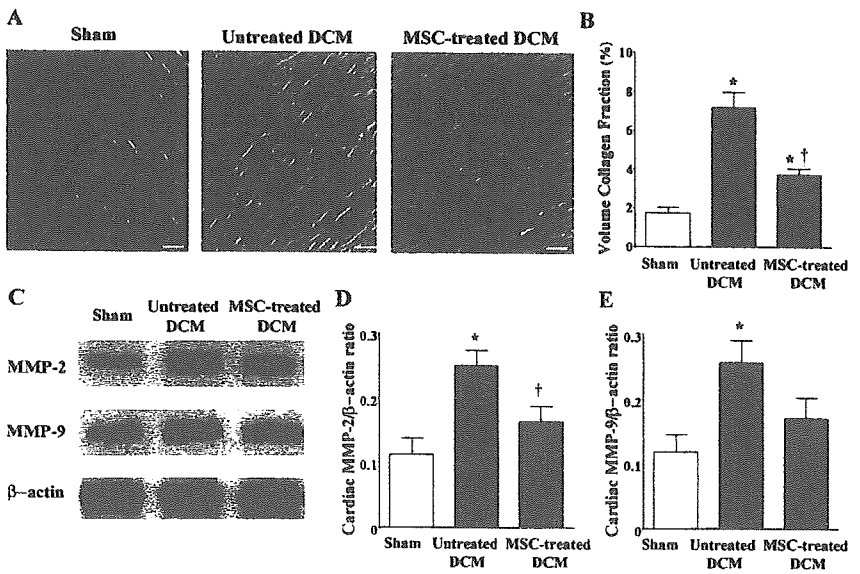

Figure 7. Effects of MSC transplantation on myocardial fibrosis. A, Photomicrographs show representative myocardial sections stained with Masson's trichrome. Scale bars=10 μm. B, Quantitative analysis demonstrated that the collagen volume fraction in the MSC-treated DCM group was significantly smaller than that in the untreated DCM group. C, Representative Western blots for MMPs-2 and -9 and β-actin in the heart. D and E, Quantitative analysis of cardiac tissue contents of MMP-2 and -9. Data are mean±SEM *$P<0.05$ vs sham group; †$P<0.05$ vs untreated DCM group.

HGF has not only angiogenic but also cardioprotective effects, including antiapoptotic, mitogenic, and antifibrotic activities.[26,27] *HGF* gene transfer into the myocardium improves myocardial function and geometry.[28] In particular, the antifibrotic effects of HGF through inhibition of transforming growth factor-β expression is beneficial for heart failure. Cultured MSCs secreted a large amount of HGF. In vivo, transplantation of MSCs slightly increased plasma HGF in rats. It significantly attenuated the development of myocardial fibrosis in a rat model of DCM. These results suggest that MSC-derived HGF may contribute to improvements in cardiac function partly through its antifibrotic effects.

MSCs also produced AM, a potent vasodilator and cardioprotective peptide.[29] We have shown that AM prevents cardiomyocyte apoptosis through the phosphatidylinositol 3-kinase/Akt–dependent pathway[16] and that it has potent angiogenic effects.[30] AM inhibits proliferation of cardiac fibroblasts through the cAMP-dependent pathway.[31] Administration of AM inhibits LV remodeling and improves cardiac function in heart failure.[32–34] In the present study, cultured MSCs secreted a large amount of AM in vitro. In vivo, transplantation of MSCs markedly increased plasma AM level. Taken together, these findings suggest that MSCs may exert their cardioprotective effects through AM-mediated paracrine regulation.

IGF-1, a growth hormone mediator, plays an important role in myocardial and skeletal muscle growth.[35,36] Administration of IGF-1 improves cardiac function after myocardial infarction through enhancement of myocardial growth.[37] Its protective and antiapoptotic properties have been demonstrated in different models of myocardial ischemia.[38] Furthermore, IGF-1 exerts Ca^{2+}-dependent, positive inotropic effects through a phosphatidylinositol 3-kinase–dependent pathway.[39] Interestingly, the present study demonstrated that MSCs secreted significant amounts of IGF-1 in vitro, 10-fold greater than MNCs. These findings raise the possibility that MSC-derived IGF-1 may participate in myocardial growth and enhancement of myocardial contractility in a rat model of DCM.

MMPs also play a crucial role in extracellular remodeling in heart failure.[40] In fact, pharmacological inhibition of MMP activities prevents progressive LV remodeling in an animal model of heart failure.[41] In the present study, cardiac MMP-2 and MMP-9 were increased in rats with DCM, which is consistent with recent findings in patients with heart failure.[40,42] Interestingly, MSC transplantation attenuated the increases in cardiac MMP-2 and MMP-9 in a rat model of DCM. Although the underlying mechanisms remain unclear, MSC transplantation may influence extracellular remodeling in heart failure.

The present study has some limitations. First, immunohistochemical evidence suggests differentiation of MSCs into cardiomyocytes, vascular endothelial cells, and smooth muscle cells. However, further studies are necessary to convincingly demonstrate differentiation of MSCs into a specific cell type. Second, the model of DCM used in this study was an injury model, and the effects of treatment may be related to attenuation of the injury rather than to the established cardiomyopathy. Nonetheless, the experiment was performed 5 to 9 weeks after myosin injection, by which time inflammatory changes were hardly observed and had been replaced by fibrosis.[43]

Conclusions

MSC transplantation improved cardiac function in a rat model of DCM, possibly through induction of myogenesis and angiogenesis, as well as by inhibition of myocardial fibrosis. The beneficial effects of MSCs may be mediated at least in part by their differentiation into cardiomyocytes and vascular cells and by their ability to supply large amounts of angiogenic, antiapoptotic, and mitogenic factors. Thus, MSC transplantation has potential as a new therapeutic strategy for the treatment of DCM.

Acknowledgments

This work was supported by research grants for cardiovascular disease (16C-6) and Human Genome Tissue Engineering 009 from the Ministry of Health, Labor and Welfare; the Industrial Technology Research Grant Program in '03 from the New Energy and Industrial Technology Development Organization of Japan; a research grant from the Japan Cardiovascular Research Foundation; and Promotion of Fundamental Studies in Health Science of the Organization for Pharmaceutical Safety and Research of Japan.

References

1. Cohn JN. The management of chronic heart failure. *N Engl J Med.* 1996;335:490–498.
2. Dec GW, Fuster V. Idiopathic dilated cardiomyopathy. *N Engl J Med.* 1994;331:1564–1575.
3. Beltrami AP, Urbanek K, Kajstura J, Yan SM, Finato N, Bussani R, Nadal-Ginard B, Silvestri F, Leri A, Beltrami CA, Anversa P. Evidence that human cardiac myocytes divide after myocardial infarction. *N Engl J Med.* 2001;344:1750–1757.
4. Pittenger MF, Mackay AM, Beck SC, Jaiswal RK, Douglas R, Mosca JD, Moorman MA, Simonetti DW, Craig S, Marshak DR. Multilineage potential of adult human mesenchymal stem cells. *Science.* 1999;284:143–147.
5. Reyes M, Dudek A, Jahagirdar B, Koodie L, Marker PH, Verfaillie CM. Origin of endothelial progenitors in human postnatal bone marrow. *J Clin Invest.* 2002;109:337–346.
6. Toma C, Pittenger MF, Cahill KS, Byrne BJ, Kessler PD. Human mesenchymal stem cells differentiate to a cardiomyocyte phenotype in the adult murine heart. *Circulation.* 2002;105:93–98.
7. Mangi AA, Noiseux N, Kong D, He H, Rezvani M, Ingwall JS, Dzau VJ. Mesenchymal stem cells modified with Akt prevent remodeling and restore performance of infarcted hearts. *Nat Med.* 2003;9:1195–1201.
8. Makino S, Fukuda K, Miyoshi S, Konishi F, Kodama H, Pan J, Sano M, Takahashi T, Hori S, Abe H, Hata J, Umezawa A, Ogawa S. Cardiomyocytes can be generated from marrow stromal cells in vitro. *J Clin Invest.* 1999;103:697–705.
9. Shake JG, Gruber PJ, Baumgartner WA, Senechal G, Meyers J, Redmond JM, Pittenger MF, Martin BJ. Mesenchymal stem cell implantation in a swine myocardial infarct model: engraftment and functional effects. *Ann Thorac Surg.* 2002;73:1919–1925.
10. Al-Khaldi A, Al-Sabti H, Galipeau J, Lachapelle K. Therapeutic angiogenesis using autologous bone marrow stromal cells: improved blood flow in a chronic limb ischemia model. *Ann Thorac Surg.* 2003;75:204–209.
11. Al-Khaldi A, Eliopoulos N, Martineau D, Lejeune L, Lachapelle K, Galipeau J. Postnatal bone marrow stromal cells elicit a potent VEGF-dependent neoangiogenic response in vivo. *Gene Ther.* 2003;10:621–629.
12. Parodi O, De Maria R, Oltrona L, Testa R, Sambuceti G, Roghi A, Merli M, Belingheri L, Accinni R, Spinelli F, Pellegrini A, Baroldi G. Myocardial blood flow distribution in patients with ischemic heart disease or dilated cardiomyopathy undergoing heart transplantation. *Circulation.* 1993;88:509–522.
13. Kodama M, Zhang S, Hanawa H, Saeki M, Inomata T, Suzuki K, Koyama S, Shibata A. Effects of 15-deoxyspergualin on experimental autoimmune giant cell myocarditis of the rat. *Circulation.* 1995;91:1116–1122.
14. Watanabe K, Ohta Y, Nakazawa M, Higuchi H, Hasegawa G, Naito M, Fuse K, Ito M, Hirono S, Tanabe N, Hanawa H, Kato K, Kodama M, Aizawa Y. Low dose carvedilol inhibits progression of heart failure in rats with dilated cardiomyopathy. *Br J Pharmacol.* 2000;130:1489–1495.

15. Nagaya N, Uematsu M, Kojima M, Ikeda Y, Yoshihara F, Shimizu W, Hosoda H, Hirota Y, Ishida H, Mori H, Kangawa K. Chronic administration of ghrelin improves left ventricular dysfunction and attenuates development of cardiac cachexia in rats with heart failure. *Circulation.* 2001;104:1430–1435.
16. Okumura H, Nagaya N, Itoh T, Okano I, Hino J, Mori K, Tsukamoto Y, Ishibashi-Ueda H, Miwa S, Tambara K, Toyokuni S, Yutani C, Kangawa K. Adrenomedullin infusion attenuates myocardial ischemia/reperfusion injury through the phosphatidylinositol 3-kinase/Akt-dependent pathway. *Circulation.* 2004;109:242–248.
17. Messina LM, Podrazik RM, Whitehill TA, Ekhterae D, Brothers TE, Wilson JM, Burkel WE, Stanley JC. Adhesion and incorporation of lacZ-transduced endothelial cells into the intact capillary wall in the rat. *Proc Natl Acad Sci U S A.* 1992;89:12018–12022.
18. Harada M, Itoh H, Nakagawa O, Ogawa Y, Miyamoto Y, Kuwahara K, Ogawa E, Igaki T, Yamashita J, Masuda I, Yoshimasa T, Tanaka I, Saito Y, Nakao K. Significance of ventricular myocytes and nonmyocytes interaction during cardiocyte hypertrophy: evidence for endothelin-1 as a paracrine hypertrophic factor from cardiac nonmyocytes. *Circulation.* 1997;96:3737–3744.
19. Ohta H, Tsuji T, Asai S, Sasakura K, Teraoka H, Kitamura K, Kangawa K. A simple immunoradiometric assay for measuring the entire molecules of adrenomedullin in human plasma. *Clin Chim Acta.* 1999;287:B131–B143.
20. Murohara T, Ikeda H, Duan J, Shintani S, Sasaki K, Eguchi H, Onitsuka I, Matsui K, Imaizumi T. Transplanted cord blood-derived endothelial precursor cells augment postnatal neovascularization. *J Clin Invest.* 2000; 105:1527–1536.
21. Tateishi-Yuyama E, Matsubara H, Murohara T, Ikeda U, Shintani S, Masaki H, Amano K, Kishimoto Y, Yoshimoto K, Akashi H, Shimada K, Iwasaka T, Imaizumi T. Therapeutic Angiogenesis using Cell Transplantation (TACT) Study Investigators. Therapeutic angiogenesis for patients with limb ischaemia by autologous transplantation of bone-marrow cells: a pilot study and a randomised controlled trial. *Lancet.* 2002;360:427–435.
22. Tse HF, Kwong YL, Chan JK, Lo G, Ho CL, Lau CP. Angiogenesis in ischaemic myocardium by intramyocardial autologous bone marrow mononuclear cell implantation. *Lancet.* 2003;4:47–49.
23. Min JY, Sullivan MF, Yang Y, Zhang JP, Converso KL, Morgan JP, Xiao YF. Significant improvement of heart function by cotransplantation of human mesenchymal stem cells and fetal cardiomyocytes in postinfarcted pigs. *Ann Thorac Surg.* 2002;74:1568–1575.
24. Kamihata H, Matsubara H, Nishiue T, Fujiyama S, Tsutsumi Y, Ozono R, Masaki H, Mori Y, Iba O, Tateishi E, Kosaki A, Shintani S, Murohara T, Imaizumi T, Iwasaka T. Implantation of bone marrow mononuclear cells into ischemic myocardium enhances collateral perfusion and regional function via side supply of angioblasts, angiogenic ligands, and cytokines. *Circulation.* 2001;104:1046–1052.
25. Kinnaird T, Stabile E, Burnett MS, Lee CW, Barr S, Fuchs S, Epstein SE. Marrow-derived stromal cells express genes encoding a broad spectrum of arteriogenic cytokines and promote in vitro and in vivo arteriogenesis through paracrine mechanisms. *Circ Res.* 2004;94:678–685.
26. Nakamura T, Nishizawa T, Hagiya M, Seki T, Shimonishi M, Sugimura A, Tashiro K, Shimizu S. Molecular cloning and expression of human hepatocyte growth factor. *Nature.* 1989;342:440–443.
27. Nakamura T, Mizuno S, Matsumoto K, Sawa Y, Matsuda H, Nakamura T. Myocardial protection from ischemia/reperfusion injury by endogenous and exogenous HGF. *J Clin Invest.* 2000;106:1511–1519.
28. Li Y, Takemura G, Kosai K, Yuge K, Nagano S, Esaki M, Goto K, Takahashi T, Hayakawa K, Koda M, Kawase Y, Maruyama R, Okada H, Minatoguchi S, Mizuguchi H, Fujiwara T, Fujiwara H. Postinfarction treatment with an adenoviral vector expressing hepatocyte growth factor relieves chronic left ventricular remodeling and dysfunction in mice. *Circulation.* 2003;107:2499–2506.
29. Kitamura K, Kangawa K, Kawamoto M, Ichiki Y, Nakamura S, Matsuo H, Eto T. Adrenomedullin: a novel hypotensive peptide isolated from human pheochromocytoma. *Biochem Biophys Res Commun.* 1993;192:553–560.
30. Tokunaga N, Nagaya N, Shirai M, Tanaka E, Ishibashi-Ueda H, Harada-Shiba M, Kanda M, Ito T, Shimizu W, Tabata Y, Uematsu M, Nishigami K, Sano S, Kangawa K, Mori H. Adrenomedullin gene transfer induces therapeutic angiogenesis in a rabbit model of chronic hind limb ischemia: benefits of a novel nonviral vector, gelatin. *Circulation.* 2004;109:526–531.
31. Tsuruda T, Kato J, Kitamura K, Kawamoto M, Kuwasako K, Imamura T, Koiwaya Y, Tsuji T, Kangawa K, Eto T. An autocrine or a paracrine role of adrenomedullin in modulating cardiac fibroblast growth. *Cardiovasc Res.* 1999;43:958–967.
32. Nishikimi T, Yoshihara F, Horinaka S, Kobayashi N, Mori Y, Tadokoro K, Akimoto K, Minamino N, Kangawa K, Matsuoka H. Chronic administration of adrenomedullin attenuates transition from left ventricular hypertrophy to heart failure in rats. *Hypertension.* 2003;42:1034–1041.
33. Nakamura R, Kato J, Kitamura K, Onitsuka H, Imamura T, Cao Y, Marutsuka K, Asada Y, Kangawa K, Eto T. Adrenomedullin administration immediately after myocardial infarction ameliorates progression of heart failure in rats. *Circulation.* 2004;110:426–431.
34. Nagaya N, Satoh T, Nishikimi T, Uematsu M, Furuichi S, Sakamaki F, Oya H, Kyotani S, Nakanishi N, Goto Y, Masuda Y, Miyatake K, Kangawa K. Hemodynamic, renal, and hormonal effects of adrenomedullin infusion in patients with congestive heart failure. *Circulation.* 2000;101:498–503.
35. Fuller J, Mynett JR, Sugden PH. Stimulation of cardiac protein synthesis by insulin-like growth factors. *Biochem J.* 1992;282:85–90.
36. Florini JR, Ewton DZ, Coolican SA. Growth hormone and the insulin-like growth factor system in myogenesis. *Endocr Rev.* 1996;17:481–517.
37. Cittadini A, Stromer H, Katz SE, Clark R, Moses AC, Morgan JP, Douglas PS. Differential cardiac effects of growth hormone and insulin-like growth factor-1 in the rat: a combined in vivo and in vitro evaluation. *Circulation.* 1996;93:800–809.
38. Li Q, Li B, Wang X, Leri A, Jana KP, Liu Y, Kajstura J, Baserga R, Anversa P. Overexpression of insulin-like growth factor-1 in mice protects from myocyte death after infarction, attenuating ventricular dilation, wall stress, and cardiac hypertrophy. *J Clin Invest.* 1997;100:1991–1999.
39. von Lewinski D, Voss K, Hulsmann S, Kogler H, Pieske B. Insulin-like growth factor-1 exerts Ca^{2+}-dependent positive inotropic effects in failing human myocardium. *Circ Res.* 2003;92:169–176.
40. Thomas CV, Coker ML, Zellner JL, Handy JR, Crumbley AJ 3rd, Spinale FG. Increased matrix metalloproteinase activity and selective upregulation in LV myocardium from patients with end-stage dilated cardiomyopathy. *Circulation.* 1998;97:1708–1715.
41. Spinale FG, Coker ML, Krombach SR, Mukherjee R, Hallak H, Houck WV, Clair MJ, Kribbs SB, Johnson LL, Peterson JT, Zile MR. Matrix metalloproteinase inhibition during the development of congestive heart failure: effects on left ventricular dimensions and function. *Circ Res.* 1999;85:364–376.
42. Spinale FG, Coker ML, Heung LJ, Bond BR, Gunasinghe HR, Etoh T, Goldberg AT, Zellner JL, Crumbley AJ. A matrix metalloproteinase induction/activation system exists in the human left ventricular myocardium and is upregulated in heart failure. *Circulation.* 2000;102:1944–1949.
43. Kodama M, Matsumoto Y, Fujiwara M, Zhang SS, Hanawa H, Itoh E, Tsuda T, Izumi T, Shibata A. Characteristics of giant cells and factors related to the formation of giant cells in myocarditis. *Circ Res.* 1991;69:1042–1050.

CLINICAL PERSPECTIVE

Transplantation of stem or progenitor cells has the potential to improve and restore cardiac function. To date, experimenters investigating the possible therapeutic effects of stem cells in the heart have used models of infarction, and little information is available about the therapeutic potential of cell transplantation for heart failure due to dilated cardiomyopathy. In the present study, we demonstrated that transplantation of stem cells improved cardiac function in a model of myocarditis. We found evidence that stem cells may work to improve heart function by both myogenesis and angiogenesis while inhibiting myocardial fibrosis. Based on our data, part of the mechanism for this improvement may occur through the action of stem cells as a source of growth factors and cytokines in the heart. This study supports the overall notion that mesenchymal stem cells transplanted into the failing heart have potential as a new therapeutic strategy for the treatment of dilated cardiomyopathy.

Circ J 2005; **69:** 1490–1495

Sustained Upregulation of Inflammatory Chemokine and Its Receptor in Aneurysmal and Occlusive Atherosclerotic Disease

—— Results From Tissue Analysis With cDNA Macroarray and Real-Time Reverse Transcriptional Polymerase Chain Reaction Methods ——

Masakazu Yamagishi, MD; Takeo Higashikata, MD*; Hatsue Ishibashi-Ueda, MD**; Hiroaki Sasaki, MD†; Hitoshi Ogino, MD†; Koji Iihara, MD††; Susumu Miyamoto, MD††; Noritoshi Nagaya, MD‡; Hitonobu Tomoike, MD; Aiji Sakamoto, MD*

Background Although cytokines are known to be pivotal in the development of atherosclerotic diseases, few data exist regarding their expressions in the established stages such as aneurysmal or occlusive lesions. Therefore, in the present study the gene expression levels of cytokine-related substances in abdominal aortic aneurysm (AAA) and carotid artery stenosis (CAS) were determined using cDNA macroarray and real-time reverse transcriptase polymerase chain reaction (RT-PCR) methods.

Methods and Results Tissue samples were obtained from 31 patients with AAA and 24 with CAS. The array-specific [^{33}P]-labeled cDNA probe mixture synthesized from 2.5μg total RNA with gene-specific primers was hybridized with nylon membranes containing 375 cDNA clones. Densitometric analysis confirmed differences in expression (>5-fold) for 97 of the cytokine-related gene products between AAA and adjacent control tissue. Among these, simultaneous upregulation was found in the expression of interleukin (IL)-8 (9-fold) and its receptor, CXCR-2 (11-fold). Thus, the expressions of IL-8 and CXCR-2 were further quantified by real-time RT-PCR. The expression of both the genes was significantly upregulated in both AAA and CAS compared with control regions as followed: IL-8=0.53±0.16 vs 0.11±0.04 ($p<0.01$); CXCR-2=2.04±0.75 vs 0.29±0.10 ($p<0.01$) in AAA, and IL-8=1.35±0.25 vs 0.60±0.16; CXCR-2=2.00±0.51 vs 0.58±0.21 ($p<0.05$) in CAS. Under these conditions, the gene expressions of monocyte chemotactic protein-1 and its receptor, CCR-2, were not significantly different in the control and diseased regions of both AAA and CAS.

Conclusions Sustained upregulation of IL-8 and CXCR-2 was observed in both AAA and CAS, suggesting the inflammatory process is still active in established dilated and occlusive atherosclerotic diseases. Whether upregulation of this system could be protective or not protective for disease development requires further study. (*Circ J* 2005; **69:** 1490–1495)

Key Words: Aneurysm; Atherosclerosis; CCR-2; Chemokines; CXCR-2; Interleukin-8

Upregulation of several genes relevant to the pathophysiology of dilated atherosclerotic diseases, such as abdominal aortic aneurysm (AAA), and stenotic diseases, such as carotid artery stenosis (CAS), has been demonstrated, particularly regarding enzymes of the matrix metalloproteinase (MMP) family and their endogenous inhibitors[1] Indeed, we previously reported that in both AAA and CAS of human tissues, upregulation of MMP genes was observed in comparison with adjacent control tissues[2,3]

In the early stage of atherosclerosis, cytokines such as monocyte chemotactic protein (MCP)-1, interleukin (IL)-6 and their receptors are overexpressed, which contributes to the initiation and development of atherosclerotic disease[4–6] However, for the established stage of these diseases when the clinical manifestations of vessel dilation or occlusion become apparent, few data exist regarding the gene expression of cytokines or chemokines in relation to overexpression of MMPs[7,8] Such evidence may contribute to our understanding of the role of cytokines and their receptors, protective or not protective, in the clinical course of vascular disease. In the present study, the gene expressions of cytokines and their receptors were systematically examined

(Received May 19, 2005; revised manuscript received August 26, 2005; accepted September 7, 2005)

*Divisions of Cardiovascular Medicine and Bioscience, *Biotechnology in Bioscience, **Pathology, †Cardiovascular Surgery, ††Neurosurgery and ‡Regenerative Medicine and Tissue Engineering, National Cardiovascular Center and Research Institute, Suita, Japan*

Part of this work was presented at the 53rd American College of Cardiology Annual Scientific Session in 2004, New Orleans, USA, and Plenary Session, 68th Annual Scientific Session of Japanese Circulation Society in 2004, Tokyo, Japan.

Mailing address: Masakazu Yamagishi, MD, PhD, FACC, Division of Cardiovascular Medicine and Bioscience, National Cardiovascular Center, 5-7-1 Fujishiro-dai, Suita 565-8565, Japan. E-mail: myamagi@hsp.ncvc.go.jp

using cDNA macroarray and then quantitatively evaluated with real-time reverse transcription polymerase chain reaction (RT-PCR) methods.

Methods

Patients and Tissue Sampling

The protocol of this study was approved by the institutional committee for ethical review. Written informed consent was given by all patients. Tissue samples were obtained from 31 patients who underwent elective graft replacement for AAA with a diameter of 58±18 mm by computed tomography (29 males, 2 females; mean age, 71±2 years) and from 24 patients who underwent carotid endarterectomy for severe stenosis (>90% diameter stenosis by angiography) of the extracranial carotid artery (all males; mean age, 68±2 years). As for medical treatment, 20 patients with AAA and 10 with CAS were treated with 3-hydroxy-3-methylglutaryl coenzyme A (HMG-CoA) reductase inhibitors, and 17 with AAA and 7 with CAS were with angiotensin-converting enzyme inhibitors or angiotensin II receptor blockade.

During graft replacement for AAA, a strip of aortic wall that contained the dilated region and relatively normal portion was carefully excised. Carotid endarterectomy was extended in a caudal direction to include a sample of minimally affected common carotid artery proximal to the plaque but in continuity with it, to act as a paired control. After removing part of the tissue for histological examination, all the samples were quickly frozen in liquid nitrogen and stored at –80°C until extraction of RNA.

RNA Preparation and cDNA Synthesis

Experimental procedures have been already described elsewhere? Briefly, the samples were homogenized in 1.0 ml ISOGEN™ reagent (Nippon Gene, Tokyo, Japan), thoroughly mixed with 0.2 ml chloroform and centrifuged at 15,000 G for 15 min at 4°C. The aqueous supernatant was transferred into a micro test tube, mixed with 0.6 ml isopropanol and centrifuged at 15,000 G for 15 min at 4°C. The precipitated total RNA was rinsed with 70% ethanol, air-dried, and then resuspended in RNase-free water. The concentration of the extracted total RNA was assessed using spectrophotometry. Next, the total RNA was treated with DNase Free™ reagent (Ambion, Austin, TX, USA) for 60 min, and then reverse-transcribed with Superscript II™ (Invitrogen, Carlsbad, CA, USA) at 37°C for 60 min using Random Primer™ (TaKaRa, Tokyo, Japan). The resultant cDNA mixture was stored in small aliquots at –20°C until further use. The integrity of each cDNA mixture was checked by amplification of glutaraldehyde 3-phosphate dehydrogenase (GAPDH) with ExTaq™ (TaKaRa), using the primer set 5'-ACCACAGTCCATGCCATCAC-3'/5'-TCCACCACCCTGTTGCTGTA-3'.

Complementary DNA Macroarray

Labeled cDNA probes were prepared with reagents provided with the Atlas Human Array kit (Clontech Laboratories, Palo Alto, CA, USA). For each specimen, 2.5 μg of total RNA was incubated with Human Cytokine-Specific Primers (R&D Systems, Minneapolis, MN, USA) for 5 min at 65°C and then at 41°C. A mixture of reaction buffer, dNTP mix, 50 U of Moloney murine leukemia virus reverse transcriptase and [α-^{32}P] dATP (Amersham Pharmacia Biotech, Piscataway, NJ, USA) was added to each sample, which was then incubated at 41°C for 60 min. The labeled cDNA probes were purified with column chromatography to remove unincorporated isotope (ProbeQuant™ G-50 Micro Columns; Amersham Pharmacia Biotech).

A nylon membrane containing bound cDNA clones corresponding to 375 different human genes (Human Cytokine Expression Array; R&D Systems) was prehybridized with a solution of hybridization buffer (ExpressHyb; Clontech) and salmon testes DNA at 68°C. Each labeled cDNA probe was mixed into prehybridization buffer and incubated overnight at 68°C with a membrane. After hybridization, the membrane was washed with wash solution 1 (2× standard saline citrate (SSC), 0.1% sodium dodecyl sulfate (SDS)) and wash solution 2 (0.1× SSC, 0.1% SDS) at 68°C followed by a final wash of 2× SSC at room temperature. The washed membrane was wrapped in plastic wrap and exposed to a phosphor imaging screen. Imaging screens were scanned and analyzed with imaging software (Atlas Image software, Clontech). The signals on each array were corrected for background with an average for blank columns and standardized with a housekeeping gene present on the same membrane (glyceraldehyde phosphate dehydrogenase). The duplicated intensity signals for each gene were summed for data analysis. The ratio of gene expression levels was determined by dividing the signal intensity on the AAA array by that on the control array. Differential gene expression was considered significant when the signal ratio was greater than 5:1.

Primers and Probes for Real-Time RT-PCR

Using Primer Express software (Applied Biosystems, Foster, CA, USA), several sets of primers were designed for each of the genes. The primer set amplifying a target cDNA most effectively, which was evaluated by electrophoresis and staining with ethidium bromide, was selected for final use. Subsequently, the TaqMan probe inherent to each primer set was prepared, which was an oligonucleotide labeled with a reporter dye (FAM) at the 5'-end and a quencher dye (TAMRA) at the 3'-end.

Real-time RT-PCR was performed using an ABI PRISM™ 7700 Sequence Detection System (Applied Biosystems). The reaction solution was assembled in a volume of 25 μl, which comprised TaqMan™ Universal PCR Master Mix (Applied Biosystems), forward and reverse primers (final concentration 300 nmol/L each), TaqMan probe (final concentration 200 nmol/L) and cDNA mixture (≈2.5 ng). The conditions for real-time RT-PCR were preheating at 50°C for 2 min and at 95°C for 10 min, followed by 40 cycles of shuttle heating at 95°C for 15 s and at 60°C for 1 min. Throughout this study, the cDNA mixture from a particular sample was used to generate the working standard for quantitation of the cDNA of interest, which plots the relationship between the dilution of the standard cDNAs and the corresponding Ct value (the number of cycles necessary to obtain a threshold fluorescent signal). The initial quantity of the cDNA of interest in a certain cDNA mixture was calculated from the working standard and then normalized to that of GAPDH determined with TaqMan™ Assay Reagent Endogenous Control (Applied Biosystems). The normalized value for each target cDNA reflects the expression level of the corresponding gene in a test sample relative to the standard tissue.

Histology and Immunohistochemistry

Part of the plaque was placed in tissue fixative